Molecular photodissociation

Shaul Mukamel and Joshua Jortner

Department of Chemistry, Tel-Aviv University, Tel-Aviv, Israel

Department of Applied Optics, Soreq Nuclear Research Centre, Yavne, Israel
(Received 5 December 1973)

In this paper we present a quantum mechanical model for direct photodissociation and for predissociation of polyatomic molecules in terms of a sequential decay scheme involving multiple coupled continua, where each continuum corresponds to a different internal vibrational state of the fragments. The coupling matrix elements between the "initial" state and the continuum states are in general determined by the appropriate vibrational overlap factors for the polyatomic radical, while intercontinua coupling for a triatomic molecule occurs only between adjacent vibrational continua. The time evolution of the system was handled by the Green's function method. Explicit theoretical expressions for the final vibrational distribution of the fragments in the photofragmentation of linear triatomic molecules were derived, which are determined by the initial coupling to the different continua and by a wave matrix which couples the various dissociative channels. The wave matrix was evaluated for some simple realistic models for the intercontinua coupling. The available experimental data for the vibrational distribution of the $CN(B^2\Sigma)$ radical resulting from photodissociation and predissociation of XCN molecules are well accounted for in terms of our theory.

I. INTRODUCTION

The basic experimental and theoretical features of direct photodissociation and predissociation of diatomic molecules are well understood since the early days of modern spectroscopy and quantum mechanics.[1–3] "Long time" optical excitation,[4] characterized by high energy resolution, of both dissociative and predissociating molecular states will result in physical information regarding the cross sections for optical absorption, for photon scattering and for photofragmentation. "Short time" excitation experiments,[5] where the excitation and the subsequent decay processes can be separated, are practical only for the case of predissociation. These will yield information regarding the time resolved decay pattern, which will be exponential for the case of a single molecular resonance when the dissociative continuum does not carry oscillator strength from the ground state, while a system characterized by a discrete zero order state coupled to an optically active continuum[6] will exhibit a complex decay pattern.[7] These general features of photofragmentation are, of course, pertinent for the elucidation of the characteristics of these processes both in diatomic and in polyatomic molecules. In the latter case additional interesting information involves the vibrational distribution of the fragments.[1f,2] In terms of quantum scattering theory this problem just corresponds to partitioning between the final open dissociative channels of the system.

The nature of the final vibrational states of the products resulting from photodissociation of triatomic molecules was considered by Holdy, Klotz, and Wilson[8a] in terms of a "half-collision" model for the atom-diatomic fragments. The ITFITS model[8b] developed later by Heidrich, Wilson, and Rapp is a direct extension of the simple "half-collision" model. Subsequently, Shapiro and Levine[9] applied the density amplitude method[10] to the "half-collision" problem to obtain the vibrational distribution of the diatomic molecules.

There are currently quite extensive experimental data available regarding the photodissociation and predissociation of triatomic XCN molecules resulting from direct optical excitation[2] and electronic energy transfer.[11] The work of Mele and Okabe[2] resulted in detailed information regarding the vibrational states of the electronically excited $CN(B^2\Sigma)$ radical obtained from photofragmentation of XCN compounds in the spectral range 2000–1300 Å. A cursory examination of the absorption spectra of ICN, BrCN, and ClCN[12] reveals that they are characterized by a broad dissociative continuum (the A system) in the 2600–1800 Å region, followed by a second weak absorption continuum towards shorter wavelengths (the α system) and an intense discrete absorption spectrum including Rydberg series below 1700 Å. Excitation into the dissociative continua corresponds to direct photodissociation, while excitation into the Rydberg bands will result in indirect photofragmentation via predissociation. It will be useful to have a general theory encompassing both kinds of processes. The "half-collision" model[8,9] does not inherently include the excitation process and so it does not define the nature of the experiment with respect to "long time" or "short time" excitation and with regard to the excited level structure. A more profound understanding of these problems will be of methodological interest. From the experimental point of view, direct photodissociation and predissociation of XCN molecules results in a vibrational distribution of the $CN(B^2\Sigma)$ radical where high vibrational levels are populated (Fig. 1). This experimental result is incompatible with the predictions of the semiclassical "half-collision" model[8] and its quantum mechanical extensions.[9]

We have recently proposed[13] that several interesting processes in electronically excited states of polyatomic molecules, such as photodissociation, predissociation, electronic quenching of an atom by a diatomic molecule[14] and vibrational excitation of diatomics via compound negative ion states,[15] are amenable to a theoretical description in terms of a sequential decay model involving multiple coupled continua. In the present paper we pre-

sent a quantum mechanical model for direct photodissociation and predissociation of polyatomic molecules, with specific applications to the dynamics of photofragmentation of triatomics.

II. A SIMPLE PHYSICAL MODEL

As became common in theoretical studies of molecular radiationless processes, we have now to define zero order states of the system and the relevant perturbation terms which couple these states. Subsequently, we have to specify the initial conditions of the system, which pertain to the "preparation" of the metastable decaying state. We shall focus attention on a general physical situation which is applicable both for direct photodissociation and for predissociation. We consider a polyatomic molecule RA, where R is a polyatomic radical and A is an atom. Adopting the conventional chemical description we consider direct photodissociation

$$RA \xrightarrow{h\nu} R + A \qquad \text{(II. 1a)}$$

and predissociation

$$RA \xrightarrow{h\nu} RA^* \rightarrow R + A\,, \qquad \text{(II. 1b)}$$

where RA is in the ground electronic state, RA* corresponds to a metastable zero order electronically excited state, while the fragments R and A may be either in the ground or in electronically excited states and the radical R may be also vibrationally excited.

The total Hamiltonian H for the system is recast in the time independent form

$$H = H_{BO} + H_v + H_{rad} + H_{int}\,, \qquad \text{(II. 2)}$$

where H_{BO} is the molecular Hamiltonian in the Born–Oppenheimer approximation, H_v represents the non adiabatic intramolecular coupling terms (i.e., nuclear kinetic energy and spin–orbit interactions), H_{rad} corresponds to the Hamiltonian of the radiation field and H_{int} denotes the molecule-radiation field interaction. The Born–Oppenheimer Hamiltonian can be represented in terms of the well known products of electronic $|j_e\rangle$ and nuclear $|j\alpha\rangle$ wavefunctions

$$|j_e\alpha\rangle \equiv |j_e\rangle\,|j\alpha\rangle \qquad \text{(II. 3)}$$

which are characterized by the zero order energies $\epsilon_{j\alpha}$, where j and α correspond to all the electronic and nuclear quantum numbers, respectively. H_{BO} takes the form

$$H_{BO} = \sum_j \sum_\alpha |j_e\alpha\rangle\,\epsilon_{j\alpha}\langle j_e\alpha| \equiv \sum_{je} |j_e\rangle\,H_{BO}^{(j)}\langle j_e|\,, \qquad \text{(II. 4)}$$

where by utilizing Eq. (II. 3) we have defined

$$H_{BO}^{(j)} \equiv \sum_\alpha |j\alpha\rangle\,\epsilon_{j\alpha}\langle j\alpha| \qquad \text{(II. 5)}$$

so that the operator $H_{BO}^{(j)}$ acts on the nuclear coordinates space.

We shall now invoke the following assumptions regarding the eigenstates of H_{BO}:

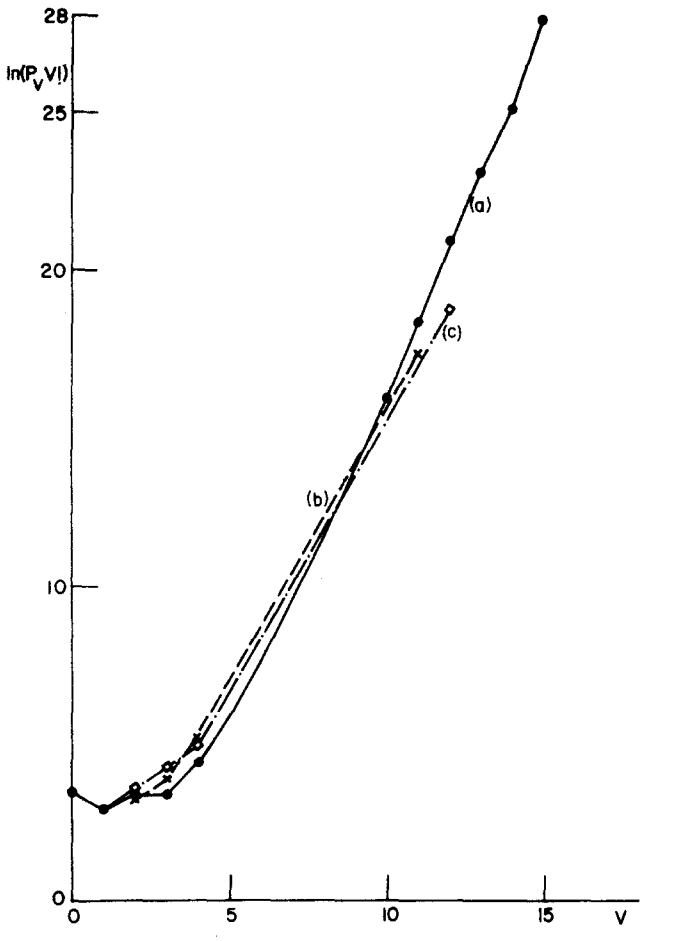

FIG. 1. The vibrational distribution P_v of the $CN(B^2\Sigma)$ radical produced by photofragmentation of various cyanides, after Mele and Okabe[2] (exciting lines 1165 Å, 1236 Å). (a) ICN; (b) BrCN; (c) ClCN. These plots should be linear for a Poissonian distribution.

(A) Only two electronic states are considered in the description of the photodissociation process, which correspond to the ground electronic state $|g_e\rangle$ and to the electronically excited dissociative continuum $|f_e\rangle$.

(B) In the case of predissociation we consider three electronic states $|g_e\rangle$, $|s_e\rangle$ and $|f_e\rangle$, where $|g_e\rangle$ and $|f_e\rangle$ are identical to those defined in (A) while $|s_e\rangle$ corresponds to a bound zero order electronically excited configuration.

(C) The operators $H_{BO}^{(g)}$ and $H_{BO}^{(s)}$ are characterized by a discrete spectrum of vibronic levels which we denote by $|g\alpha\rangle$ and $|s\beta\rangle$, respectively.

(D) The vibrational eigenfunctions $|g\alpha\rangle$ and $|s\beta\rangle$ in the $|g_e\rangle$ and $|s_e\rangle$ electronic configurations, respectively, will be represented in terms of products of harmonic oscillator functions corresponding to the normal modes of the radical R and the R–A bond mode. So that we write for the eigenfunctions of $H_{BO}^{(g)}$ and $H_{BO}^{(s)}$

$$|g\alpha\rangle = \chi_{\alpha_R}^{(g)}(\mathbf{Q}_R)\cdot\chi_{\alpha_A}^{(g)}(Q_A) \qquad \text{(II. 6a)}$$

and

$$|s\beta\rangle = \chi_{\beta_R}^{(s)}(\mathbf{Q}_R)\cdot\chi_{\beta_A}^{(s)}(Q_A)\,, \qquad \text{(II. 6b)}$$

respectively. Here $\mathbf{Q}_R$ represents the collection of the

normal modes of the R fragment and Q_A corresponds to the R–A coordinate. $\chi^{(g)}$ and $\chi^{(s)}$ correspond to bound harmonic oscillator wave functions in the two electronic states. In (II. 6) we have separated the quantum numbers α and β into α_R, and β_R which are the collections of of quantum numbers related to the R normal modes, and into α_A, and β_A which correspond to the quantum numbers of the dissociating mode. Thus

$$\alpha \equiv (\alpha_R,\ \alpha_A) \tag{II. 7a}$$

and

$$\beta \equiv (\beta_R,\ \beta_A)\ . \tag{II. 7b}$$

The representation (II. 6) corresponds to a quasidiatomic approximation for these bound states.

(E) The potential for the nuclear motion in the dissociative $|f_e\rangle$ electronic state is represented in terms of a sum of contributions of the molecular fragment R and the interaction between R and the atom A. Thus $H_{BO}^{(f)} = T + V^{(f)}$, where T is the nuclear kinetic energy and

$$V^{(f)}(\mathbf{Q}_R, Q_A) = V_R(\mathbf{Q}_R) + V_{RA}(Q_A)\ , \tag{II. 8}$$

where $\mathbf{Q}_R$ is the collection of the internal nuclear coordinates of R while Q_A is the single dissociative coordinate. The interaction potential (II. 8) involves contributions only from neighboring atoms.

(F) The potential $V_R(\mathbf{Q}_R)$ is harmonic.

(G) The role of bending modes and of rotations will be disregarded and we consider at present a linear dissociation process along Q_A.

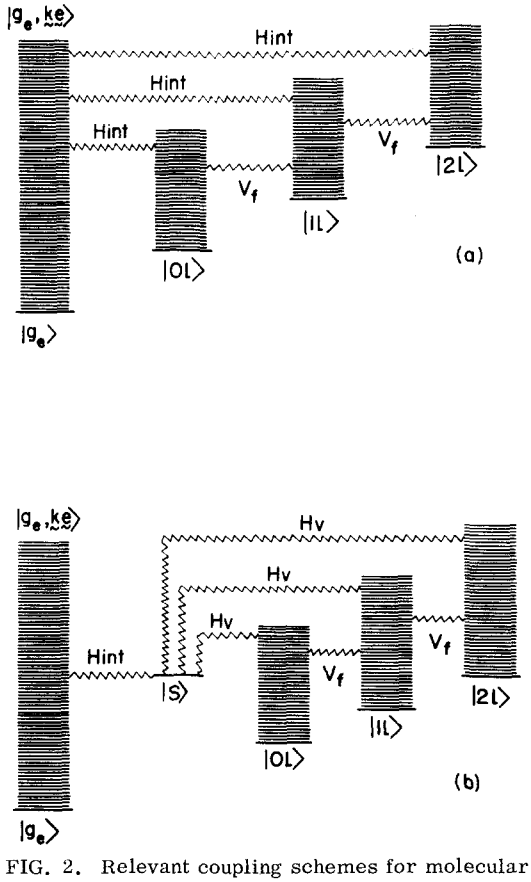

FIG. 2. Relevant coupling schemes for molecular fragmentation (a) Direct photodissociation, (b) predissociation.

(H) The Hamiltonian $H_{BO}^{(f)}$ for nuclear motion in the $|f_e\rangle$ state is represented in the form

$$H_{BO}^{(f)} = \overline{H}_{BO}^{(f)} + V_f\ . \tag{II. 9}$$

The eigenstates of $\overline{H}_{BO}^{(f)}$ are given in terms of a product of harmonic oscillator wavefunctions of the internal coordinates of the polyatomic fragment R, and a function of the dissociative coordinate Q. Thus these zero order nuclear eigenstates $|f\gamma\rangle$, with the eigenvalues $\epsilon_{f\gamma}$, are given by

$$|f\gamma\rangle = \chi_{\gamma_R}^{(f)}(\mathbf{Q}_R) \cdot \chi_l^{(f)}(Q_A)\ . \tag{II. 10a}$$

And so

$$\overline{H}_{BO}^{(f)} = \sum_{\gamma} |f\gamma\rangle\, \epsilon_{f\gamma} \langle f\gamma|\ , \tag{II. 10b}$$

where $\chi_{\gamma_R}^{(f)}$ is the nuclear wavefunction (product of harmonic oscillators) which corresponds to the radical R characterized by the vibrational quantum numbers γ_R, while $\chi_l^{(f)}$ corresponds to the dissociative mode, and is specified by the quantum number l for the relative translational energy in the latter mode. The nuclear perturbation term V_f consists of mixed derivatives with respect to nuclear coordinates and it is completely defined in terms of Eqs. (II. 5), (II. 9), and (II. 10). We note in passing that the basis (II. 10) does not correspond to the Born–Oppenheimer nuclear wavefunctions (in the harmonic approximation) but rather to a more crude representation. This representation is, however, more general than the simple "quasidiatomic approximation" utilized[1a] to describe the line shape of dissociative spectra of polyatomics, which did not include the perturbation term V_f.

We shall now utilize Eqs. (II. 2), (II. 4), (II. 5), and (II. 9) to partition the total Hamiltonian in the general form

$$H = H_0 + V\ . \tag{II. 11}$$

For the case of direct photodissociation we consider a two electronic level system

$$H_0 = |g_e\rangle H_{BO}^{(g)} \langle g_e| + |f_e\rangle \overline{H}_{BO}^{(f)} \langle f_e| + H_{rad}\ , \tag{II. 12}$$

$$V = H_{int} + |f_e\rangle V_f \langle f_e| \tag{II. 13}$$

while for the case of predissociation, three electronic configurations are included,

$$H_0 = |g_e\rangle H_{BO}^{(g)} \langle g_e| + |s_e\rangle H_{BO}^{(s)} \langle s_e| + |f_e\rangle \overline{H}_{BO}^{(f)} \langle f_e| + H_{rad}\ , \tag{II. 14}$$

$$V = H_{int} + H_v + |f_e\rangle V_f \langle f_e|\ . \tag{II. 15}$$

Now, as we are not interested in multiphoton processes we limit our attention to weak electromagnetic fields, and thus consider only zero photon, $|\mathrm{vac}\rangle$, eigenstates and one photon, $|\mathbf{ke}\rangle$, eigenstates of H_{rad}. Here $\mathbf{k}$ specifies the wave vector and $\mathbf{e}$ is the polarization vector of a photon. The zero order eigenstates of H_0 (Eqs. (II. 12) and (II. 14) are: $|g_e\alpha, \mathbf{ke}\rangle$ and $|f_e\gamma, \mathrm{vac}\rangle$ for photodissociation and $|g_e\alpha, \mathbf{ke}\rangle$, $|s_e\beta, \mathrm{vac}\rangle$, and $|f_e\gamma, \mathrm{vac}\rangle$ for predissociation. The molecular wave functions are specified in terms of Eqs. (II. 3), (II. 6), and (II. 10). A

schematic energy levels diagram for photodissociation and predissociation is portrayed in Fig. 2.

To avoid unnecessary formal manipulations let us now specify the experimental conditions for both experiments. We shall be mainly interested in the vibrational distribution of the fragments [i.e., the states γ_R, see Eq. (II.10)] resulting from direct or indirect photodecomposition. In the case of direct photodissociation we can consider excitation of the molecule by a photon wavepacket $\sum_{\mathbf{ke}} a_{\mathbf{ke}} |\mathbf{ke}\rangle$, where the coefficients $a_{\mathbf{ke}}$ represent the wavepacket amplitudes, so that the state of the system at $t=0$ is

$$|g\rangle \equiv \psi(0) = \sum_{\mathbf{ke}} a_{\mathbf{ke}} |g_e 0, \mathbf{ke}\rangle \ , \tag{II.16}$$

where $\alpha = 0$ corresponds to the lowest vibrational level of the ground electronic state.

The excitation amplitudes $a_{\mathbf{ke}}$ determine the time scale of our experiment.[16,17]

In a typical "long excitation" experiment we have a monochromatic field (i.e., $a_{\mathbf{ke}} = \delta(\mathbf{k}-\mathbf{k}_0)\,\delta(\mathbf{e}-\mathbf{e}_0)$) and we can envision the photodissociation as a scattering of $|g\rangle \equiv |g_e \alpha, \mathbf{ke}\rangle$ into a set of coupled continua $|f_e \gamma, \text{vac}\rangle$. To specify the vibrational distribution of the products we have to evaluate the elements of the scattering S matrix, which may be obtained as the limit $t \to \infty$ of the matrix elements of the time evolution operator $U(-t/2, t/2)$.[16] In order to monitor the time dependence of a photodissociating system we should begin with a photon wave packet of finite width.

In the case of predissociation we assume that the dissociative continuum does not carry oscillator strength from the ground state and the only appreciable coupling by H_{int} is between the $|g_e \alpha, \mathbf{ke}\rangle$ and $|s_e \beta, \text{vac}\rangle$ states. The line shape for each predissociating state is a Lorentzian characterized by a total width $\gamma_{s\beta}$ provided that the spacings between different $|s\beta\rangle$ levels exceed the widths of the resonances. We can then consider the excitation of the molecule by a light pulse of duration $\tau_p \ll \gamma_{s\beta}^{-1}$. Under these conditions we can consider the time evolution of an initially excited state[16,17]

$$|g\rangle \equiv |s_e \beta, \ \text{vac}\rangle \tag{II.17}$$

decaying nonradiatively into a set of coupled continua $|f_e \gamma, \text{vac}\rangle$.

From the foregoing discussion we conclude that we can finally describe both direct photodissociation and predissociation in terms of a two electronic levels system characterized by the decay of a single resonance state $|g\rangle$ given in terms of Eqs. (II.16) or (II.17) into the coupled manifolds $|f\rangle \equiv |f_e \gamma, \text{vac}\rangle$. The relevant coupling matrix elements of the perturbation (II.13) or (II.15) between these zero order states are of course different for the two cases.

For the case of direct photodissociation we have

$$V_{g,f\gamma} \equiv \langle g_e \alpha, \mathbf{ke} | H_{\text{int}} | f_e \gamma, \text{vac}\rangle \ , \tag{II.18}$$

$$V_{f\gamma, f\gamma'} \equiv \langle f_e \gamma, \text{vac} | V_f | f_e \gamma', \text{vac}\rangle \ . \tag{II.19}$$

Making use of Eqs. (II.6), and (II.10) and invoking the Condon approximation, the coupling matrix elements (II.18) take the explicit form:

$$V_{g\alpha, f\gamma} = K \cdot h(k) \langle g_e | \mathbf{p}\cdot\mathbf{e} | f_e \rangle \cdot (\chi_{\alpha_R}^{(g)}(\mathbf{Q}_R) | \chi_{\gamma_R}^{(f)}(\mathbf{Q}_R)) \cdot (\chi_{\alpha_A}^{(g)}(Q_A) | \chi_l^{(f)}(Q_A)), \tag{II.20}$$

where $\langle\ \rangle$ and $(\ )$ denote matrix elements in the electronic and nuclear coordinates space, respectively, and where

$$K = -(e\hbar/m)(2\pi/Q\hbar c)^{1/2} \ . \tag{II.20'}$$

Here e and m denote the electron charge and mass respectively, c is the velocity of light, and Q is the volume of the system (note that our photon states are box normalized). $h(k) = 1/\sqrt{k}$ contains the dependence of the coupling on the photon energy. The $\langle g_e | \mathbf{p}\cdot\mathbf{e} | f_e \rangle$ factor is an electronic matrix element of the electronic momentum (in the direction of the photon polarization $\mathbf{e}$). The product $(\chi_{\alpha_A}^{(g)}(Q_A) | \chi_l^{(f)}(Q_A))$ corresponds to the vibrational overlap integral between the harmonic R–A mode in the ground state and the dissociative R–A mode in the excited state, while

$$FC_{gf}(\alpha_R, \gamma_R) \equiv (\chi_{\alpha_R}^{(g)}(\mathbf{Q}_R) | \chi_{\gamma_R}^{(f)}(\mathbf{Q}_R)) \tag{II.21}$$

corresponds to the Franck–Condon vibrational-overlap integral between the harmonic modes of the R fragment in the two electronic states. These are determined by the configurational modifications and frequency changes between the ground state of the molecule and the resulting R radical.

Let us consider a photon polarized parallel to the molecular electronic transition matrix element $\langle g_e | \mathbf{p} | f_e \rangle$ then for a given bound-continuum electronic transition the product

$$D_l^{(\text{pd})} \equiv Kh(k) \langle g_e | \mathbf{p}\cdot\mathbf{e} | f_e \rangle (\chi_{\alpha_A}^{(g)}(Q_A) | \chi_l^{(f)}(Q_A)) \tag{II.22}$$

depends essentially only on the quantum number l of the dissociative mode, and we finally write for the case of photodissociation

$$V_{g\alpha, f\gamma} = D_l^{(\text{pd})} \cdot FC_{gf}(\alpha_R, \gamma_R) \ . \tag{II.22'}$$

In the derivation of Eq. (II.22') we have assumed that we begin with $\alpha_A = 0$ (ground vibronic level) and we have also ignored the weak k dependence of $h(k)$. It should be noted that calculation of absolute cross sections requires averaging of (II.22) over molecular orientations.

Turning now to the case of predissociation, the coupling matrix elements between the zero order states are

$$V_{g, f\gamma} = \langle s_e \beta, \text{vac} | H_v | f_e \gamma, \text{vac}\rangle \ , \tag{II.23}$$

while $V_{f\gamma, f\gamma'}$ is again given by Eq. (II.19). When the electronic configurations $|s_e\rangle$ and $f_e\rangle$ correspond to different spin states $H_V = H_{\text{so}}$ is the spin–orbit coupling operator, whereupon (II.23) takes the form

$$V_{g, f\gamma} = D_l^{(\text{so})} FC_{gf}(\alpha_R, \gamma_R) \ , \tag{II.24}$$

where

$$D_l^{(\text{so})} = \langle S_e | H_{\text{so}} | f_e \rangle (\chi_0^{(g)}(Q_A) | \chi_l^{(f)}(Q_A)) \tag{II.25}$$

and $FC_{gf}(\alpha_R, \gamma_R)$ is given by Eq. (II.21). Equation (II.24) for spin orbit induced predissociation is, of course, analogous to Eq. (II.22). When nonadiabatic

coupling between the same spin states $|s_e\rangle$ and $|f_e\rangle$ is considered Eq. (II. 23) is rather complex. A reasonable approximation is based on the assumption that the major contribution to nuclear kinetic energy coupling originates from the dissociative coordinate, whereupon we define the double vibrational electronic integral

$$D_l^{(na)} = \left(\chi_0^{(g)}(Q_A)\,\langle s_e \mid \frac{\partial}{\partial Q_A}\,|f_e\rangle\,\chi_l^{(f)}(Q_A)\right) \qquad \text{(II. 25')}$$

and

$$V_{g,f\gamma} \cong D_l^{(na)}\,FC_{gf}(\alpha_R, \gamma_R)\ . \qquad \text{(II. 26)}$$

We thus conclude that the coupling matrix elements (II. 18) and (II. 23) between the "initial" state and the continuum states are determined by the Franck–Condon overlap (II. 21) both for the case of photodissociation and for predissociation. What remains to be done is to obtain explicit expressions for the coupling matrix elements (II. 19) connecting different continuum states which correspond to different vibrational states of the R fragment. This will be done for the case of a triatomic molecule.

III. INTERCONTINUUM COUPLING FOR A TRIATOMIC MOLECULE

We consider now the V_f operator for the linear photodissociation or predissociation of the triatomic molecule ABC, resulting in the diatomic fragment BC and the atom A. Equation (II. 8) takes the form

$$V^{(f)} = V_{AB}(R_{AB}) + V_{BC}(R_{BC})\ , \qquad \text{(III. 1)}$$

where R_{AB} and R_{BC} are the internuclear distances, V_{AB} is repulsive, and V_{BC} is harmonic. Making use of the reduced coordinates[10]

$$y = \left[\frac{(\mu_{BC}\bar{k})^{1/2}}{\hbar}\right]^{1/2}(R_{BC} - \bar{R}_{BC})\ , \qquad \text{(III. 2)}$$

$$x = \left[\frac{(\mu_{BC}\bar{k})^{1/2}}{\hbar}\right]^{1/2}\left[\frac{m_B + m_C}{m_C}\,\tilde{X} - \bar{R}_{BC}\right]$$

and of the reduced mass parameter

$$m = \frac{m_A m_C}{(m_A + m_B + m_C)m_B} \qquad \text{(III. 3)}$$

the nuclear Hamiltonian (II. 5) for the dissociative state takes the form[10]

$$H_{BO}^{(f)} = -\frac{1}{2m}\,\frac{\partial^2}{\partial x^2} - \frac{1}{2}\,\frac{\partial^2}{\partial y^2} + \frac{1}{2}\,y^2 + V(x-y)\ , \qquad \text{(III. 4)}$$

where $V(x-y)$ is a repulsive term. In Eq. (III. 2) and (III. 3) $\bar{k}, \bar{R}_{BC}$, and μ_{BC} are the BC oscillator force constant, equilibrium distance, and reduced mass, respectively. R_{BC} is the BC distance and $\tilde{X}$ is the distance of A from the center of mass of the BC molecule. Note that Eq. (III. 4) is mathematically equivalent to the Schrödinger equation of a particle of mass m colliding with a harmonic oscillator of unit mass. We can now define a new coordinate $z = (x-y)$ and transform Eq. (III. 4) to a new set of coordinates (y, z), whereupon

$$H_{BO}^{(f)} = -\frac{1}{2m}\,\frac{\partial^2}{\partial z^2} - \frac{1}{2}\left(1 + \frac{1}{m}\right)\frac{\partial^2}{\partial y^2} + \frac{1}{2}\,y^2 + V(z) - \frac{1}{m}\,\frac{\partial^2}{\partial y\,\partial z} \qquad \text{(III. 5)}$$

Thus Eq. (II. 5) is dissected as follows:

$$\bar{H}_{BO}^{(f)} = -\frac{1}{2m}\,\frac{\partial^2}{\partial z^2} - \frac{1}{2}\left(1 + \frac{1}{m}\right)\frac{\partial^2}{\partial y^2} + \frac{1}{2}\,y^2 + V(z)\ , \qquad \text{(III. 6)}$$

$$V_f = -\frac{1}{m}\,\frac{\partial^2}{\partial y\,\partial z} \qquad \text{(III. 7)}$$

so that the intercontinua coupling involves a product of the nuclear momenta for the internal BC coordinate and for the dissociative z coordinate. The eigenstates of $\bar{H}_{BO}^{(f)}$ Eq. (II. 6), for the present case are

$$|f_e\gamma\rangle \equiv \chi_v^{(f)}(y)\,\chi_l^{(f)}(z)\ , \qquad \text{(III. 8)}$$

where v is the vibrational quantum number of the diatomic fragment BC and l represents the relative translational energy in the z dissociative mode. For the sake of convenience we shall denote the set of dissociative continua in the triatomic molecule by

$$|vl\rangle \equiv |f_e\gamma, \text{vac}\rangle\ . \qquad \text{(III. 9)}$$

The relevant zeroth energy levels scheme is given in Fig. 2. To explore the detailed form of the intercontinua matrix elements (II. 19) with V_f given by Eq. (III. 7) and the states represented in terms of Eqs. (III. 8) and (III. 9), we write

$$V_f = -\frac{1}{\sqrt{2}\,m}\,(a - a^+)\,\frac{\partial}{\partial z}\ , \qquad \text{(III. 10)}$$

where a and a^+ correspond to the annihilation and to the creation operators of the $B-C$ oscillator. Thus Eq. (II. 19) takes the form

$$V_{vl,v'l'} \equiv \langle vl \mid V_f \mid v'l'\rangle = -\frac{1}{\sqrt{2}\,m}\,\langle v|(a - a^+)|v'\rangle\langle l \mid \frac{\partial}{\partial z}\,|l'\rangle\ . \qquad \text{(III. 11)}$$

We note in passing that (III. 11) vanishes for $v = v'$. For the sake of convenience we choose the $|l\rangle$ wavefunctions to be real (sinusoidal behavior at large z). Let us consider $|l\rangle$ to be the wavefunctions of a particle in a box. In this case we have

$$\langle l \mid \frac{\partial}{\partial z}|l'\rangle \sim \frac{ll'}{l^2 - l'^2}\ , \ l + l' = 2n+1$$
$$\sim 0\ , \qquad l + l' = 2n\ . \qquad \text{(III. 12)}$$

We then assume that our matrix elements of $\partial/\partial z$ behaves in a similar way, i.e.,

$$\langle l|\,\partial/\partial z\,|l'\rangle = C_{ll'}\ , \quad l > l'$$
$$= -C_{l'l}\ , \quad l < l'\ . \qquad \text{(III. 13)}$$

Now, since we are interested in near resonance coupling between $|g\rangle$ [Eq. (II. 6)] and the continua $\{|vl\rangle\}$, we have to consider the $\{|vl\rangle\}$ states in the vicinity of $|g\rangle$. This implies that we can utilize Eq. (III. 13) with $l > l'$ for $v < v'$ and with $l < l'$ for $v > v'$. Thus from Eqs. (III. 11) and (III. 13) we get

$$\langle vl \mid V_f \mid v'l'\rangle = \langle v \mid -\frac{1}{\sqrt{2}\,m}\,(C_{ll'}a + C_{l'l}a^+)\,|v'\rangle \qquad \text{(III. 14)}$$

Making use of the well known properties of a and a^+,

$$\langle v|a|v'\rangle = \sqrt{v+1}\,\delta_{v',v+1}\ , \tag{III.15}$$

$$\langle v|a^+|v'\rangle = \sqrt{v}\,\delta_{v',v-1}\ , \tag{III.16}$$

we now obtain the general form of the coupling matrix elements

$$V_{vl,v'l'} = \langle vl|V_f|v'l'\rangle = \sqrt{v+1}\,\alpha_{ll'}\,\delta_{v',v+1} + \sqrt{v}\,\alpha_{l'l}\,\delta_{v',v-1}\ , \tag{III.17}$$

where we have defined

$$\alpha_{ll'} = -(1/\sqrt{2}\,m)\,C_{ll'}\ . \tag{III.18}$$

Equation (III.17) implies that intercontinuum coupling in the photofragmentation of triatomics occurs only between adjacent continua. This is a consequence of the harmonic approximation for the diatomic BC radical, which is explicit in Eq. (III.4).[18]

Finally we have to specify the coupling matrix elements $V_{g,vl}$ [see Eqs. (II.18) and (II.23)] for the linear photodissociation or predissociation of a triatomic molecule. From Eqs. (II.22), (II.24), and (II.26) we write

$$V_{g,vl} = D_l^{(i)} FC(v)\ ;\quad i = \mathrm{pd},\ \mathrm{so},\ \mathrm{na} \tag{III.19}$$

where $FC(v)$ corresponds to the Franck–Condon vibrational overlap integral for the BC mode. Denoting by η the dimensionless reduced shift in the BC harmonic mode between the ground state and the diatomic radical, and assuming that in the ground state, only the zero vibrational level is populated we have

$$V_{g,vl} = D_l^{(i)} \exp\left(-\frac{\eta^2}{4}\right)\left(\frac{\eta}{\sqrt{2}}\right)^v \Big/ \sqrt{v!}\ . \tag{III.20}$$

If the initial state is characterized by a vibrational quantum number v_s (not necessarily zero) we have:

$$V_{g(v_s),vl} = D_l^{(i)} \exp\left(-\frac{\eta^2}{4}\right)\sqrt{v_s!\,v!} \otimes \sum_{r=0}^{\min(v,v_s)} (-1)^{v-r}\,\frac{(\eta/\sqrt{2})^{v+v_s-2r}}{r!\,(v_s-r)!\,(v-r)!}\ . \tag{III.21}$$

Equation (III.21) is important particularly for predissociation where the different initial vibrational states may be selected by optical excitation. We could have easily extended Eqs. (III.20) and (III.21) to incorporate the frequency change in the BC mode, however this is not essential at present.

In conclusion we notice that the relevant coupling terms (III.17) and (III.20) between zero order states in the photodissociation and predissociation of a triatomic molecule are determined by the parameters $\alpha_{ll'}$, $D_l^{(i)}$ and the cofigurational change η.

IV. SEQUENTIAL DECAY MODEL FOR PHOTOFRAGMENTATION

Photodissociation and predissociation in polyatomic molecules can be now theoretically described in terms of a sequential decay scheme[19] where the $|g\rangle$ state [Eqs. (II.16), (II.17)] is coupled to a set of continua, each corresponding to a different internal vibrational state of the fragments, and where different continua are coupled. A model system for sequential decay has been recently handled by Nitzan *et al.*[19] who derived a general solution for the case when the intercontinua coupling matrix elements are constant. We shall now consider the case of sequential decay for a triatomic molecule (Fig. 2) considering the decay of the $|g\rangle$ state into the manifold, $\{|vl\rangle\}$ $(v = 0, 1, \ldots, N-1)$.

The time evolution of the system will be handled by the Green's function method. Let the matrix elements of the Green's function $G^+(E) = (E - H + i\eta)^{-1}$, $\eta \to 0^+$, be denoted by $G^+_{ij}(E)$, where $i, j \equiv g, vl$. Then the probability to find the system in the "initial" state is

$$p_g(t) = \frac{1}{4\pi^2}\left|\int_{-\infty}^{+\infty} \exp(-iEt)\,G^+_{gg}(E)\,dE\right|^2 \tag{IV.1}$$

while the probability of decay into the v continuum is obtained by summation over all the states in this particular continuum

$$p_v(t) = \frac{1}{4\pi^2}\sum_l \left|\int_{-\infty}^{+\infty} \exp(-iEt)\,G^+_{vl,g}(E)\,dE\right|^2 . \tag{IV.2}$$

The final vibrational distribution of the fragments is

$$p_v \equiv p_v(\infty)\ . \tag{IV.3}$$

The problem is reduced to the evaluation of the matrix elements of the Green's function, which can be accomplished by the application of the Dyson equation,[5] resulting in

$$G^+_{gg} = \frac{1}{E^+ - E_g} + \frac{1}{E^+ - E_g}\sum_v\sum_l V_{g,vl}\,G^+_{vl,g} \tag{IV.4}$$

$$G^+_{vl,g} = \frac{1}{E^+ - E_{vl}}\sum_{v'}\sum_{l'} V_{vl,v'l'}\,G^+_{v'l',g} + \frac{1}{E^+ - E_{vl}}\,V_{vl,g}\,G^+_{gg} \tag{IV.5}$$

for each v and l, where $E_i (i = g, vl)$ are the energies of the zero order states, and $E^+ \equiv E + i\eta$.

Equations (IV.4) and (IV.5) provide us with an infinite set of coupled algebraic equations. In order to obtain manageable results the following approximations are introduced at this stage:

(I) The number N of the continua is finite, being determined by the highest continuum accessible by resonance coupling to $|g\rangle$ (see Fig. 2).

(J) The coupling matrix elements $V_{g,vl}$ are independent on the particular translational state l, and we set $D_l^{(i)} = D$ in Eq. (III.19). Thus $V_{g,vl} = V_{g,v}$ being determined by the Franck–Condon overlap. [We take the continuum states to be energy normalized, i.e., $\langle l|l'\rangle = \delta(l - l')$.] This simplifying assumption, which will result in the vanishing of some level shift terms due to the $g \leftrightarrow vl$ coupling, is common in the treatment of radiative and non radiative coupling with continua.

(K) The intercontinua coupling terms [Eq. (III.17)] will be simplified by assuming that the coefficients $\alpha_{ll'}$ in Eq. (III.18) are independent of the particular translational states. Since we are essentially interested in near resonance coupling it is reasonable to assume that $\alpha_{ll'}$ for the coupling between $\{|vl\rangle\}$ and $\{|v+1, l\rangle\}$ is

determined by the continuum index v, and we shall replace $\alpha_{ll'}$ by $\alpha^{(v)}$. For the present we shall even go further and assume that $\alpha^{(v)}$ is independent of v. This last assumption will be relaxed in Sec. V.

(L) The dissociative continua are unbound below, and threshold corrections will be disregarded. This assumption is consistent with assumptions (J) and (K), and will result in the vanishing of level shift terms.

Invoking assumptions (I) and (K) we may now rewrite Eqs. (IV.4) and (IV.5) as follows:

$$G^+_{gg} = \frac{1}{E^+ - E_g}\left(1 + \sum_v \sum_l V_{g,vl} G^+_{vl,g}\right) , \tag{IV.6}$$

$$G^+_{vl,g} = (E^+ - E_{vl})^{-1}\Big(\alpha^{(v+1)}\sqrt{v+1} \sum_{l'} G^+_{(v+1)l',g} + \alpha^{(v)}\sqrt{v} \sum_{l'} G^+_{(v-1)l',g}\Big) + (E^+ - E_{vl})^{-1} V_{vl,g} G^+_{gg} , \tag{IV.7}$$

where $v = 0, 1, \ldots, N-1$ and $0 < (l, l') < \infty$. Note also that in Eq. (IV.7)

$$\alpha^{(0)} = \alpha^{(N)} = 0 . \tag{IV.8}$$

We now perform an integration over the continuum states, $\sum_l \to \int dE_l \rho_l^{(v)}$, where $\rho_l^{(v)}$ is the density of states in the $\{|vl\rangle\}$ continuum. We define the sums

$$A_v \equiv \sum_l G^+_{vl,g} = \int dE_l \rho_l^{(v)} G^+_{vl,g} . \tag{IV.9}$$

Utilizing assumption (L) we obtain from (IV.7) the set of equations

$$A_v = -i\pi\rho_l^{(v)}(\alpha^{(v+1)}\sqrt{v+1}\, A_{v+1} + \alpha^{(v)}\sqrt{v}\, A_{v-1}) - i\pi\rho_l^{(v)} V_{v,g} G^+_{gg} \tag{IV.10}$$

for $v = 0, 1, \ldots, N-1$, and where

$$A_N = A_{-1} = 0 . \tag{IV.10'}$$

In deriving Eq. (IV.10) we have used the relation

$$\int_{-\infty}^{+\infty} \frac{\rho_l^{(v)} dE_l}{E^+ - E_{vl}} = -i\pi\rho_l^{(v)} \tag{IV.11}$$

the (real) principal part of the integral (IV.11) was disregarded.

Finally, utilizing assumption (J) we recast Eqs. (IV.6) in the form

$$(E^+ - E_g) G^+_{gg} = 1 + \sum_v V_{g,v} A_v \tag{IV.12}$$

while Eq. (IV.7) takes the form

$$G^+_{vl,g} = (E^+ - E_{vl})^{-1}[\alpha^{(v+1)}\sqrt{v+1}\, A_{v+1} + \alpha^{(v)}\sqrt{v}\, A_{v-1} + V_{v,g} G^+_{gg}] . \tag{IV.13}$$

Equations (IV.10) and (IV.12) constitute a set of $N+1$ algebraic equations for $A_0, A_1, \ldots, A_{N-1}$ and G^+_{gg}, once this set of equations is solved we obtain an explicit expression for $G^+_{vl,g}$ via Eq. (IV.13).

We have previously provided the solution of these equations for the simplest possible case where the intercontinua coupling terms are constant being independent both of v and of l.[13] We shall now proceed in two steps. First we consider the effect of the internal coupling contributions $\sqrt{v}$ and $\sqrt{v+1}$ on the intercontinua coupling terms. In Sec. V we first present a solution assuming that $\alpha^{(v)}$ is independent on v. Later we present the solution for some simplified but physically reasonable v dependence of $\alpha^{(v)}$.

V. APPROXIMATE SOLUTIONS FOR THE SEQUENTIAL DECAY PROBLEM

We now proceed to derive an explicit solution for Eqs. (IV.10) and (IV.12). In the treatment presented in this section we assume that the coefficients $\alpha^{(v\pm1)}\rho_l^{(v)}$ are constant, independent of v, thus we may omit the superscripts from these quantities. We have thus the following set of $N+1$ equations:

$$A_v = \beta\sqrt{v+1}\, A_{v+1} - \beta^*\sqrt{v}\, A_{v-1} - \gamma_v , \quad v = 0, 1, \ldots, N-1 \tag{V.1}$$

$$(E^+ - E_g) G^+_{gg} = 1 + \sum_v V_{g,v} A_v , \tag{V.2}$$

where

$$A_{-1} = A_N = 0 . \tag{V.3}$$

Here we have defined the parameter β which corresponds to the reduced intercontinuum coupling

$$\beta = -i\pi\alpha\rho_l , \qquad \beta^* = i\pi\alpha\rho_l , \tag{V.4}$$

and

$$\gamma_v = i\pi V_{v,g}\rho_l G^+_{gg} . \tag{V.5}$$

The off-diagonal elements $G^+_{vl,g}$ are given by Eq. (IV.13) with

$$\alpha^{(v+1)} = \alpha^{(v)} = \alpha . \tag{V.6}$$

A. Coupling of $|g\rangle$ with a single continuum

We shall consider first the simple case of coupling of the "initial" state to a single continuum $\{|kl\rangle\}$ so that

$$V_{g,v} = V_{g,k}\delta_{v,k} . \tag{V.7}$$

Equations (V.1), (V.2) takes the form

$$A_v = \beta\sqrt{v+1}\, A_{v+1} - \beta^*\sqrt{v}\, A_{v-1} , \quad v \neq k \tag{V.8}$$

$$A_k = \beta\sqrt{k+1}\, A_{k+1} - \beta^*\sqrt{k}\, A_{k-1} - \gamma_k \tag{V.9}$$

$$(E^+ - E_g) G^+_{gg} = 1 + V_{g,k} A_k . \tag{V.10}$$

The solution of the set of Eqs. (V.8)–(V.10) is represented in the form (see Appendix A)

$$A_v = -F(v,k)\cdot\gamma_k , \tag{V.11}$$

where the matrix $F(v,k)$ is defined as follows:

$$F(v,k) \equiv \frac{Q_v \bar{Q}_k}{Q_N}\left(\frac{k!}{v!}\right)^{1/2}\beta^{k-v}, \quad v \leq k$$

$$\equiv \frac{Q_k \bar{Q}_v}{Q_N}\left(\frac{v!}{k!}\right)^{1/2}(-\beta^*)^{v-k} , \quad v \geq k . \tag{V.12}$$

The matrix $F(v,k)$ is determined in terms of the Q_v and $\bar{Q}_v$ polynomials, defined and listed in Appendix A. From Eqs. (V.8), (V.9), and (V.11) it follows that it obeys the recurrence relation

$$F(v,k)=\beta\sqrt{v+1}\,F(v+1,k)-\beta^*\sqrt{v}\,F(v-1,k)+\delta_{v,k}\,. \tag{V.13}$$

The diagonal matrix element of the Green's function [Eq. (V.10)] can be now expressed utilizing Eq. (V.11),

$$G^+_{gg}(E)=(E-E_g+(i/2)\Gamma_{gk})^{-1}\,, \tag{V.14}$$

where the characteristic width is

$$\Gamma_{gk}=2\pi(Q_k\overline{Q}_k/Q_N)\,|\,V_{g,k}\,|^2\rho_l \tag{V.15}$$

which can be finally written in the form

$$\Gamma_{gk}=\Gamma^0_{gk}F(k,k) \tag{V.16}$$

and where the zeroth width is defined as

$$\Gamma^0_{gk}\equiv 2\pi\,|\,V_{g,k}\,|^2\rho_l\,. \tag{V.16'}$$

We now proceed to the evaluation of the the off-diagonal matrix elements of the Green's function [Eq. (IV.7)]. Making use of Eq. (V.11) we obtain:

$$G^+_{vl,g}=\frac{-\gamma_k}{E^+-E_{vl}}\,[\alpha\sqrt{v+1}\,F(v+1,k)+\alpha\sqrt{v}\,F(v-1,k)]$$

$$+\frac{V_{v,g}}{E^+-E_{vl}}\,G^+_{gg}\sigma_{v,k}\,. \tag{V.17}$$

Application of Eqs. (V.5), (V.13), and (V.14) to (V.17) results in

$$G^+_{vl,g}(E)=\frac{F(v,k)\,V_{kg}}{(E-E_g+i\Gamma_{gk}/2)(E^+-E_{vl})}\,. \tag{V.18}$$

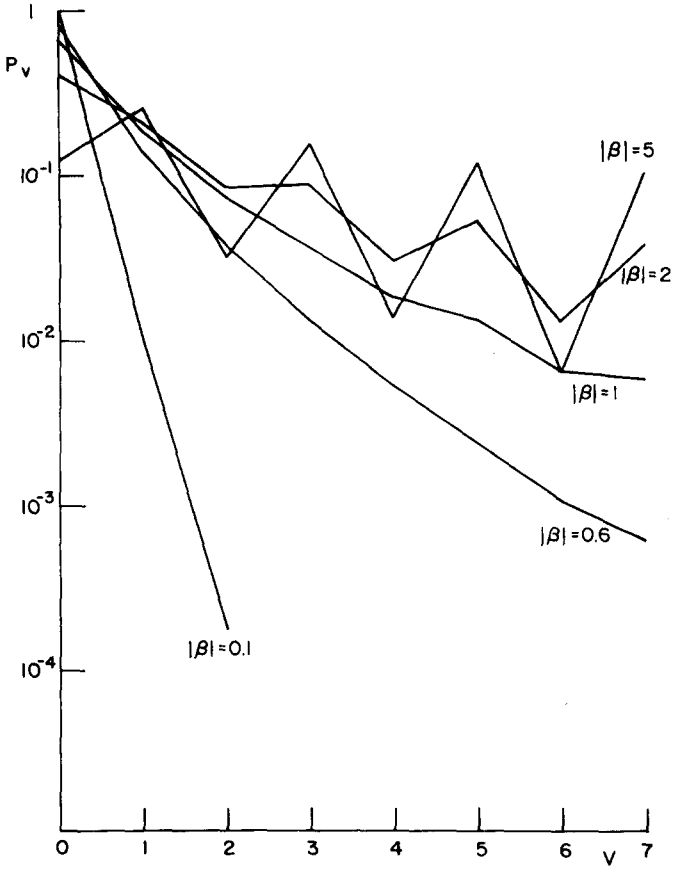

FIG. 3. Vibrational distribution of products [Eq. (V.21)] for various $|\beta|$ values. $N=14$, $k=0$.

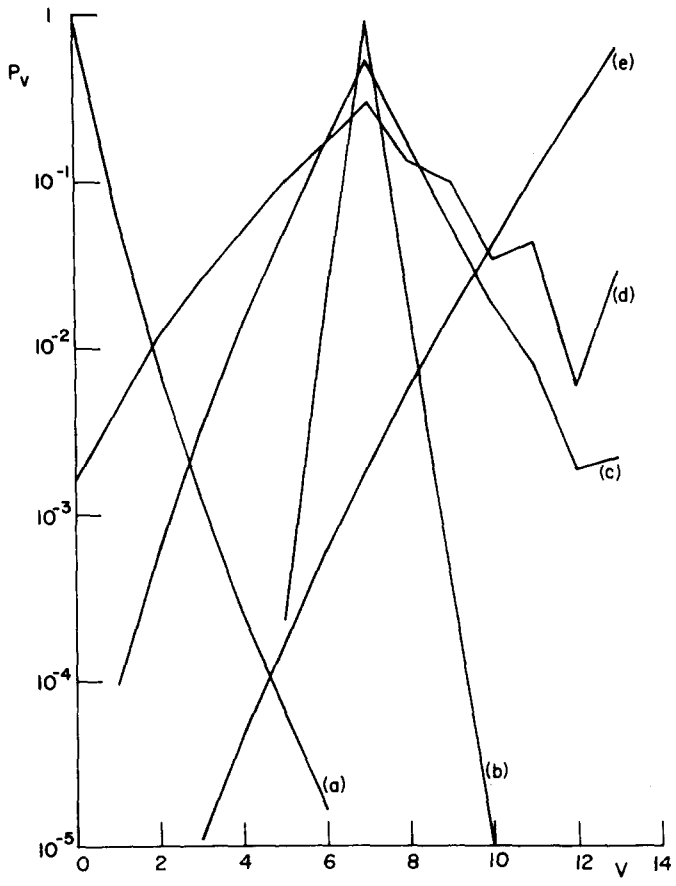

FIG. 4. Dependence of the vibrational distribution on the initial vibrational state k and the coupling parameter β for $N=14$ in the weak coupling limit. (a) $k=0$ $|\beta|=0.3$, (b) $k=7$ $|\beta|=0.05$, (c) $k=7$ $|\beta|=0.3$, (d) $k=7$ $|\beta|=0.6$, (e) $k=13$ $|\beta|=0.3$.

Equations (V.14) and (V.18) together with the definitions (V.12) and (V.16) determine the time evolution of the system. Making use of the general relations (IV.1), (IV.2) we obtain for the present case

$$P_g(t)=|\,C_g(t)\,|^2=\exp(-\Gamma_{gk}t) \tag{V.19}$$

$$|\,C_{vl}(t)\,|^2=\frac{|\,F(v,k)\,|^2\,|\,V_{k,g}\,|^2}{(E_l-E_g)^2+\Gamma^2_{gk}/4}\{1+\exp(-\Gamma_{gk}t)$$

$$-2\exp(-\Gamma_{gk}t/2)\cos[(E_l-E_g)\,t]\}\,. \tag{V.20}$$

The probability (IV.2) for the decay into the v continuum at $t=\infty$ is

$$P_v=\int\,|\,C_{vl}(\infty)\,|^2\rho_l\,dE_l=|\,F(v,k)\,|^2\,. \tag{V.21}$$

The matrix $F(v,k)$ contains all the relevant physical information regarding the time evolution of the system characterized by $|g\rangle \rightleftharpoons |kl\rangle$ coupling. We notice that "the decay width" Γ_{gk} is determined by the diagonal elements $F(k,k)$, while the vibrational partitioning is given in terms of $|\,F(v,k)\,|^2$.

The **F** matrix is determined by the polynomials Q_v and $\overline{Q}_v$ [via Eq. (V.12)]. These polynomials include the same powers in $|\,\beta\,|^2$ for the pairs Q_{2m}, Q_{2m+1} and $\overline{Q}_{2m}$, $\overline{Q}_{2m-1}$, where m is an integer, $m\leq(N-1)/2$. Thus the degree of the Q_v polynomials increases while the degree of the $\overline{Q}_v$ polynomials decreases by two for every second polynomial (see Appendix A). We also note that

F obeys the unitary conservation relation

$$\sum_v |F(v,k)|^2 = 1 \ . \qquad \text{(V.21')}$$

It will be useful at this stage to explore the implications for the model system with $|g\rangle \longleftrightarrow |kl\rangle$ coupling:

(a) For the limit of weak intercontinua coupling $|\beta| \ll 1$ and the polynomials Q_v and $\bar{Q}_v$ are close to unity for all v.

In this limit we have from Eqs. (V.12), (V.21)

$$P_v = |\beta|^{2(v-k)}(v!/k!), \quad v \geq k$$
$$= |\beta|^{-2(v-k)}(k!/v!), \quad v \leq k \ . \qquad \text{(V.22)}$$

We note in passing that only when $k = N-1$ (i.e., for direct coupling to the last continuum) the distribution is Poissonic. The vibrational distribution is then a smooth function of v, as demonstrated in Fig. 3 for the physically relevant case $k=0$ [i.e., $\eta \approx 0$ in Eq. (III.20)].

(b) In the limit of strong intercontinua coupling when $|\beta| \gtrsim 1$ the vibrational distribution exhibits an oscillatory steplike structure, (see Fig. 3) which originates from a significant contribution of the polynomials Q_v and $\bar{Q}_v$ to $F(v,k)$. The increase in an even power of $|\beta|$ for every second polynomial results in an oscillatory distribution in the strong coupling limit for the model used herein. This feature of the distribution arises from our assumption (K) of constant coupling strength between all the continua and will be relaxed in Sec. VB.

(c) The k dependence of the distribution is presented in Figs. 4 and 5. In the weak coupling situation P_v exhibits a maximum at $v=k$ followed by a sharp decrease (of the form $|\beta|^{2|v-k|}$ for $|\beta| \ll 1$) at higher v. In the strong coupling limit the distribution is less regular.

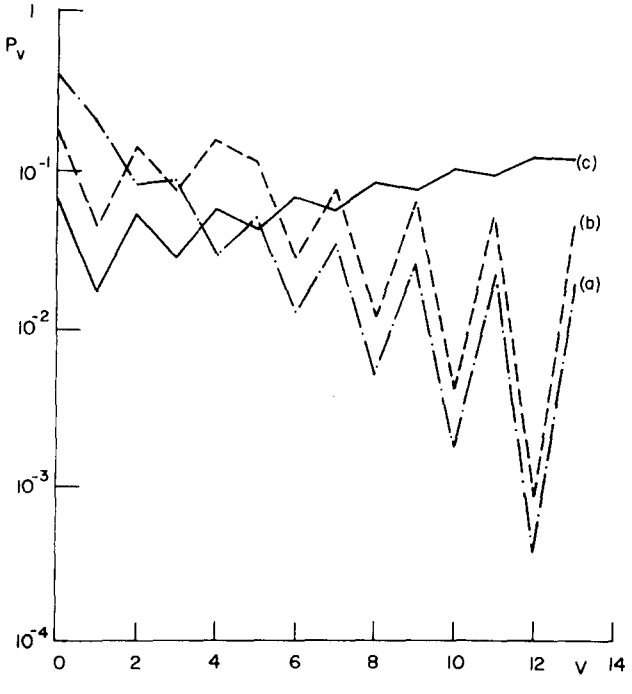

FIG. 5. Dependence of the vibrational distribution on the initial vibrational state k and the coupling parameter β for $N=14$ in the strong coupling limit. $|\beta| = 2$. (a) $k=0$, (b) $k=5$, (c) $k=13$.

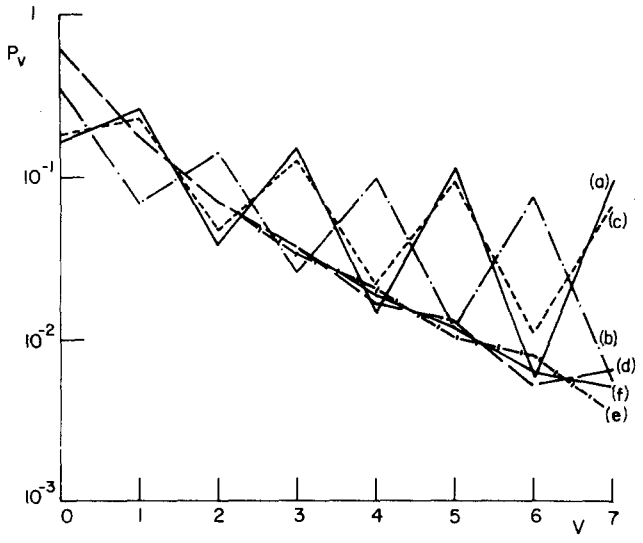

FIG. 6. Dependence of the vibrational distribution P_v on the number of continua (N). Strong coupling, $|\beta| = 4$ (a) $N=12$, (b) $N=15$, (c) $N=16$. Weak coupling, $|\beta| = 1$. (d) $N=12$, (e) $N=15$ (f) $N=16$.

(d) The dependence of $P_v(\infty)$ on N is weak for $|\beta| \lesssim 1$ (when v is not too close to N), and also for $|\beta| \gg 1$ for either even or for odd N values. We note that changing N by unity in the strong coupling case shifts the maxima and minima in $P_v(\infty)$ from v to $v+1$ (see Fig. 6). In this case the averaged distribution:

$$\langle P_v \rangle = [P_v^{(N)}(\infty) + P_v^{(N+1)}(\infty)]/2 \qquad \text{(V.23)}$$

is a smooth function of v. This averaged $\langle P_v \rangle$ distribution exhibits a weak dependence on N.

(e) All the results deduced so far pertain both for predissociation and photodissociation. In the case of predissociation we can identify Γ_{gk} with the decay rate of the "initially prepared" $|g\rangle$ state, whose decay mode is exponential [see Eq. (V.19)].

(f) The width Γ_{gk} decreases with increasing $|\beta|$ (Fig. 7). This is a manifestation of the role of interference effects in sequential decay, which was previously studied

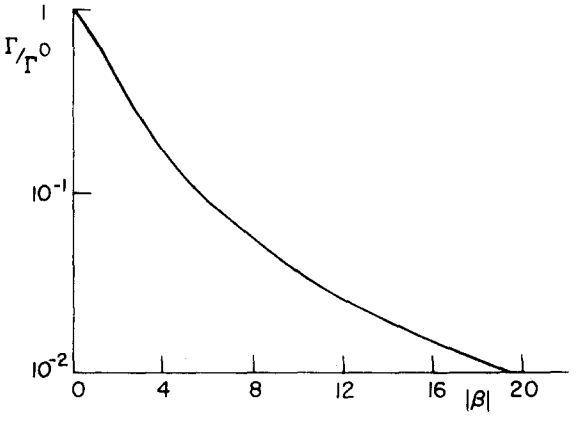

FIG. 7. Retardation of the characteristic width [Eq. (V16)] as a function of $|\beta|$. $N=14$, $k=0$.

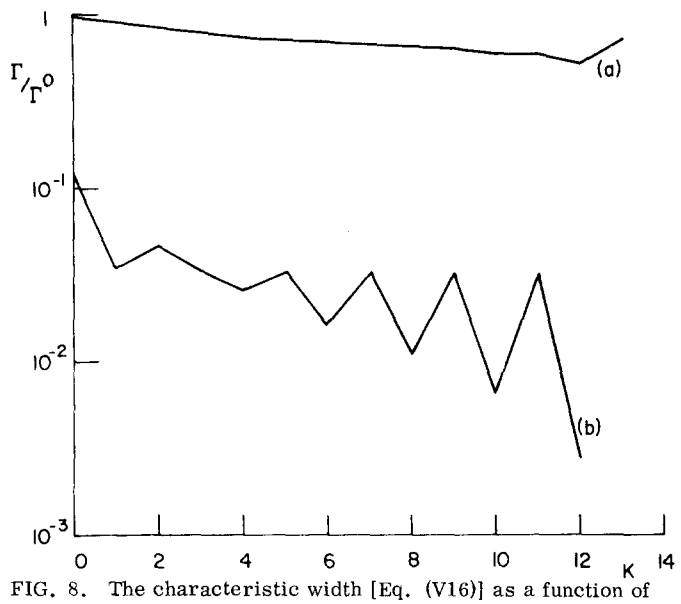

FIG. 8. The characteristic width [Eq. (V16)] as a function of k. (a) $|\beta| = 0.2$, (b) $|\beta| = 5$.

for simpler systems.[13,19] From Fig. 7 it is evident that $\Gamma_{gk} \to \Gamma^0_{gk}$ for $|\beta| \to 0$ and $\Gamma_{gk} \to 0$ for $|\beta| \gg 1$. Finally we notice that as $F(k,k)$ contains the factor $Q_k \overline{Q}_k / Q_N$ then in the strong coupling limit Γ_{gk} exhibits an oscillatory dependence on k (see Fig. 8).

(g) The results obtained herein are qualitatively similar to but differ quantitatively (see Fig. 9) from those of our previous treatment[13] of a simpler model system where the $\sqrt{v}$ dependence in Eq. (III. 17) was not included.

B. Coupling of $|g\rangle$ to all continua

Utilizing the results of Sec. (V. A) it is now possible to solve the problem [Eqs. (IV. 4) and (IV. 5) which corresponds to the initial coupling of $|g\rangle$ to all continua. Now the coupling matrix elements $V_{vl,g}$ are determined by the Franck–Condon overlaps [via Eqs. (III. 19), (III. 20)] being determined by the parameter η. The general solution for the coefficient A_v [Eq. (V. 1)] can be expressed as a superposition of the coefficients (V.11) which correspond to the special case of $|g\rangle \longleftrightarrow |kl\rangle$ coupling. Thus in the general case

$$A_v = -\sum_{k=0}^{N-1} F(v,k)\gamma_k \ . \qquad \text{(V. 24)}$$

In order to evaluate G^+_{gg} [Eq. (V. 2)] we calculate the sum

$$\sum_v V_{g,v} A_v = -\sum_v \sum_k V_{g,v} F(v,k)\gamma_k$$

$$= -i\pi\rho_l \sum_k \sum_v V_{g,v} F(v,k) V_{k,g} G^+_{gg} \ , \qquad \text{(V. 25)}$$

where we have made use of the definition (V. 5). Equation (V. 2) is now obtained in the explicit form

$$G^+_{gg} = [E - E_g - D_g + (i/2)\Gamma_g]^{-1} \ , \qquad \text{(V. 26)}$$

where we have defined the level shift D_g, and the general width Γ_g in terms of the relation

$$D_g - (i/2)\Gamma_g \equiv -i\pi\rho_l \sum_v \sum_k V_{g,v} F(v,k) V_{k,g} \ . \qquad \text{(V. 27)}$$

Defining the row vector

$$\mathbf{V} = \begin{pmatrix} V_{0g} \\ V_{1g} \\ \vdots \\ V_{N-1,g} \end{pmatrix} \qquad \text{(V. 28)}$$

of the initial coupling terms, and the matrix $\mathbf{F} = \{F(v,k)\}$ we can write

$$\Gamma_g = 2\pi \mathrm{Re}[(\mathbf{V}^+ \mathbf{F}\, \mathbf{V})\rho_l] \qquad \text{(V. 29a)}$$

and

$$D_g = \pi \mathrm{Im}[(\mathbf{V}^+ \mathbf{F}\, \mathbf{V})\rho_l] \ . \qquad \text{(V. 29b)}$$

It is now a simple matter to evaluate the off-diagonal matrix elements $G^+_{vl,g}$ which are given by Eq. (IV. 13) with $\alpha^{(v)} = \alpha$. Making use of Eq. (V. 24) we get

$$G^+_{vl,g} = (E^+ - E_{vl})^{-1}\Big[-\alpha\sqrt{v+1}\sum_k F(v+1,k)\gamma_k$$

$$-\alpha\sqrt{v}\sum_k F(v-1,k)\gamma_k + V_{vl,g} G^+_{gg}\Big] . \qquad \text{(V. 30)}$$

Utilizing the definition (V. 5) and the recurrence relation (V. 13) we obtain

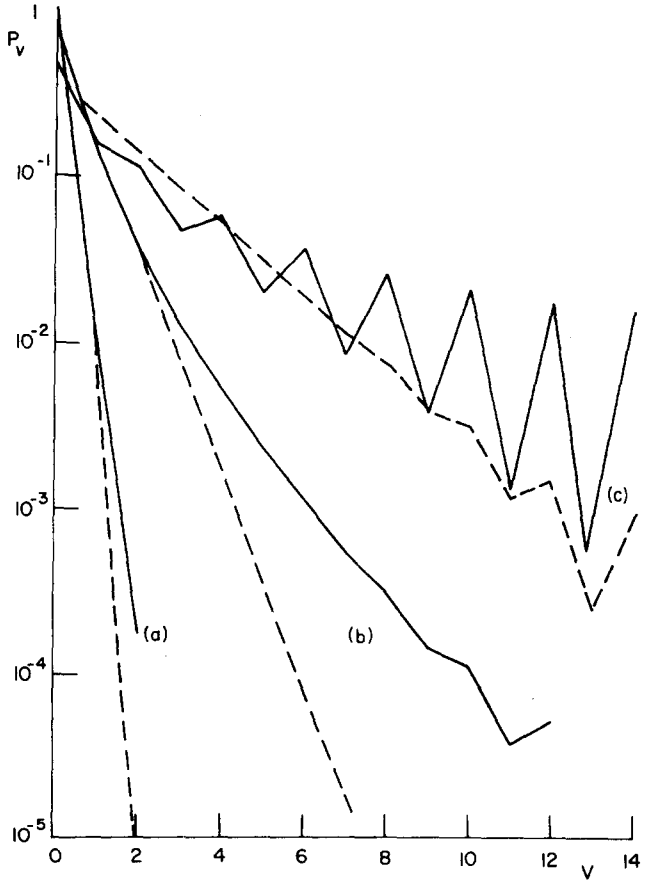

FIG. 9. The effect of the v dependence of the intercontinua coupling on the vibrational distribution. —This work (including the v depencence). - - - - Ref. 13, where the intercontinua coupling is assumed to be v independent. (a) $|\beta| = 0.1$, (b) $|\beta| = 0.6$, (c) $|\beta| = 2$.

$$G^{+}_{vl,g} = (E^{+} - E_{vl})^{-1} \sum_{k} F(v,k)\, V_{k,g}\, G^{+}_{gg}\,, \qquad \text{(V.31)}$$

with G^{+}_{gg} now given by Eqs. (V.23), (V.28), and (V.29). Thus we get

$$G^{+}_{vl,g} = \frac{\sum_k F(v,k) v_{k,g}}{[E - D_g + (i/2)\Gamma_g](E^{+} - E_{vl})}\,. \qquad \text{(V.32)}$$

The time evolution of the system is again given in terms of Eqs. (IV.1), (IV.2) together with (V.26) and (V.32). Thus, for the case of coupling of $|g\rangle$ to all the continua we get

$$P_g(t) = \exp(-\Gamma_g t) \qquad \text{(V.33)}$$

with Γ_g being given in terms of Eq. (V.29). In a similar manner we get

$$|C_{vl}(t)|^2 = \frac{|\sum_k F(v,k) V_{kg}|^2}{(E_l - E_g)^2 + \frac{1}{4}\Gamma_g^2} \times [1 + e^{-\Gamma_g t} - 2e^{-1/2\Gamma_g t}\cos(E_{vl} - E_g)t] \qquad \text{(V.34)}$$

while the final vibrational distribution takes the form

$$P_v = (2\pi/\Gamma_g)\left|\sum_k F(v,k) V_{k,g}\right|^2 \rho_l\,. \qquad \text{(V.35)}$$

We shall now define the row vector of the vibrational distributions

$$\mathbf{P} = \begin{pmatrix} P_0 \\ P_1 \\ \vdots \\ P_{N-1} \end{pmatrix} \qquad \text{(V.36)}$$

which from Eq. (V.35) and (V.27) is given in the form

$$P_v = \frac{|(\mathbf{F}\cdot\mathbf{V})_v|^2}{\mathrm{Re}(\mathbf{V}^{+}\,\mathbf{F}\,\mathbf{V})}\,. \qquad \text{(V.37)}$$

Equations (V.12) and (V.37) constitute the solution for the model system under consideration where $|g\rangle$ is coupled to all the continua. The solution is determined by the vector **V**, which specifies the initial distribution and by the **F** matrix (which is connected with the Moller wave operator) defined within the subpart of the Hilbert space spanned by the states $\{|vl\rangle\}$. We shall demonstrate elsewhere the general formal relation between Γ_g [Eq. (V.29a)] and **F V** and the projections of the level shift operator in different subparts of the Hilbert space.[20]

We shall now explore the effect of the initial coupling terms on the final vibrational distribution. The vector **V** is determined by the appropriate Franck–Condon factors via Eq. (III.20). These vibrational overlap factors are determined by the parameter η. The following points should be noticed:

(a) In Figs. 10A and 10B we present the final vibrational distribution for different η values for both weak and for strong intercontinua coupling. For small values of $\eta(\eta = 0 - 0.5)$ the distribution is insensitive to η being close to the result obtained for initial coupling to $v = 0$ only, i.e., $V_{g,v} = V_{g,0}\,\delta_{0,v}$. For large η values, the final distribution is, of course, appreciably affected by changing η.

(b) The final distribution P_v assumes a Poissonic distribution in the extreme weak coupling limit when $|\beta| \to 0$. Under these circumstances $F(v,k) = \delta_{k,v}$, and thus from Eq. (V.35) $P_v \propto |V_{v,g}|^2$ and the final distribution is then just determined by the initial coupling terms. The Poissonic distribution thus obtained in the extreme weak coupling situation originates from a different physical picture than the mathematically identical distribution obtained from the "half collision" model.[8] In the latter case the parameter of the distribution is deter-

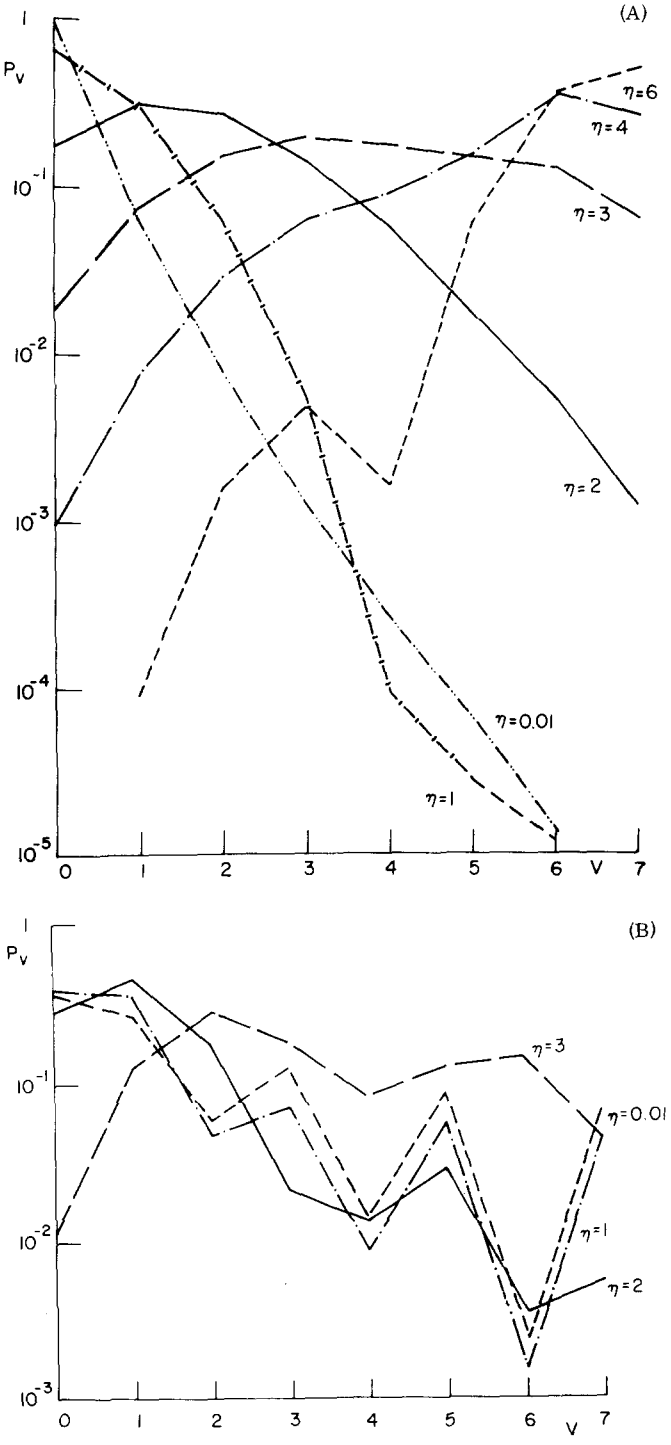

FIG. 10. The effect of η [Eq. (III.20)] on the vibrational distribution [Eq. (V.37)]. $N = 8$. (A) Weak coupling $|\beta| = 0.3$. (B) Strong coupling $|\beta| = 2$.

mined by the Fourier transform of the force exerted on the oscillator while in the present case η is related to the initial coupling.

(c) The oscillations of P_v in the strong coupling limit exist also for large η (see Fig. 10B).

(d) In the weak coupling limit the distribution is again insensitive to N for constant $|\beta|$ and η. In the strong coupling limit the averaged distribution, (averaged over two N values of different parity), which is given by Eq. (V. 23), exhibits a weak N dependence.

(e) Figure 11 portrays the dependence of P_v on the vibrational quantum number k of the initial state $|g\rangle$. This dependence is relevant for the case of predissociation where one can often select k by appropriate excitation conditions. The coupling $V_{g,vl}$ in this case is given by Eq. (III. 21). We note that k has an appreciable effect on the final vibrational distribution.

(f) The width Γ_g [Eq. (V. 29a)] decreases with increasing η (see Fig. 12). This is a consequence of interference effects, which become more pronounced when the initial coupling encompasses more states.

We were thus able to provide an explicit solution for the problem of sequential decay involving multiple continua with nearest neighbor intercontinua coupling. In our model the vibrational distribution is determined by the parameters β [Eq. (V. 4)] and η [Eq. (III. 21)]. The

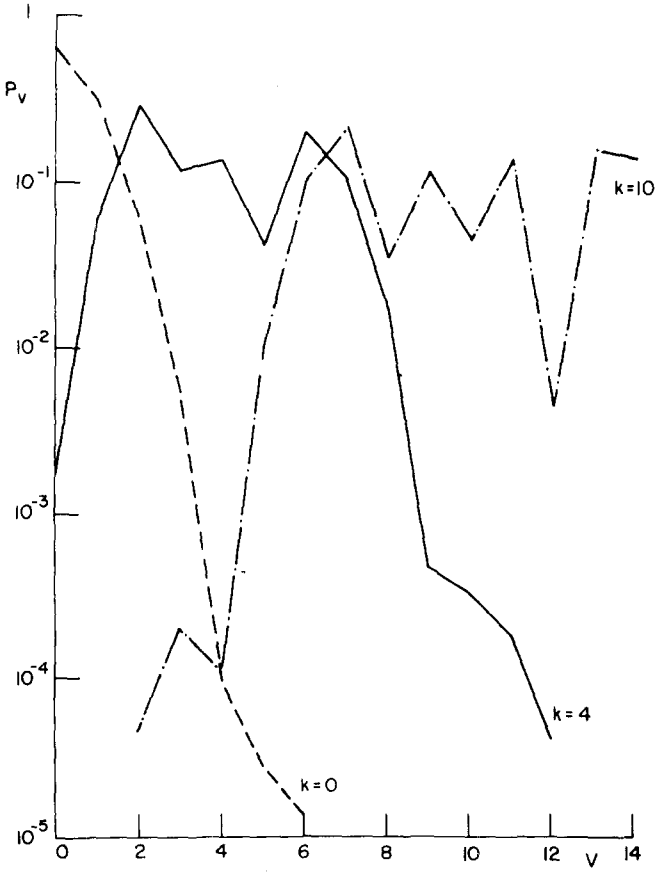

FIG. 11. Dependence of the vibrational distribution on the initial vibrational state (k) when $\eta \neq 0$ [Eqs. (III. 21), (V. 37)] $N=15$, $\eta=1$, $|\beta|=0.3$.

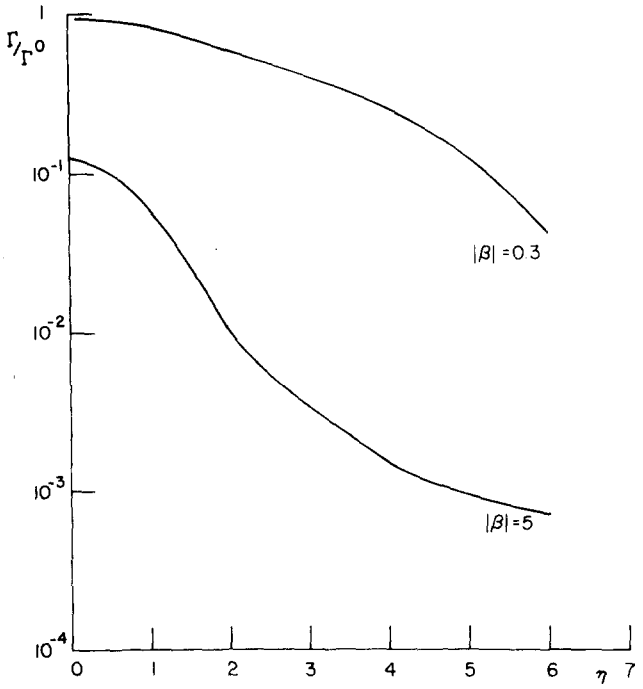

FIG. 12. The characteristic width as a function of η [Eq. (V. 29a)] $N=14$. [Γ^0 is the width assuming $|\beta|=0$ and $F(v,k)=\delta_{v,k}$].

basic simplifying assumption employed by us involves the independence of the intercontinuum coupling on the translational quantum numbers l and l' in adjacent continua. We believe that the strong oscillations exhibited in P_v for the strong coupling situations are a consequence of this assumption. Simple model calculations for the coupling between continua indicate that resonance coupling of the states $|vl\rangle$ and $|v'l'\rangle$ around the energy $E_{vl} \sim E_{v'l'} \sim E_g$ will decrease with increasing v.[21] For $v=N-1$, near threshold, we expect that $\langle N-1, l|V|N-2, l'\rangle$ will be small. The simplest way to account for this effect is to consider the intercontinuum coupling to be different for each pair of continua (v, v') (where $v'=v\pm1$). We have accordingly performed further model calculations solving Eqs. (IV. 6) and (IV. 7) and assuming that the coupling terms exhibit some specific dependence on v.

We have considered two simple cases which exhibit the attenuation of the intercontinua coupling with increasing v. First, we have taken for the intercontinua coupling terms

$$\alpha^{(v,v+1)} = \alpha_0 \exp(-\phi v) \ , \qquad \alpha^{(v,v-1)} = \alpha_0 \exp[-\phi(v-1)] \ , \tag{V. 38}$$

where $\phi > 0$ is a real number and α_0 denotes the coupling strength. The form (V. 38) corresponds to an exponential attenuation of the coupling. Second, we have used a simple linear form for the attenuation of the intercontinuum coupling

$$\alpha^{(v,v+1)} = \alpha_0 \left(1 - \frac{q}{N-2} v\right) \ , \qquad \alpha^{(v,v-1)} = \alpha_0 \left[1 - \frac{q}{N-2}(v-1)\right] \ . \tag{V. 39}$$

Here, again, α_0 represents the coupling strength and $0<q<1$ is a real number denoting the degree of attenuation. Thus $\xi=1-q$ corresponds to the ratio between $\alpha^{(N-2,N-1)}$ and $\alpha^{(0,1)}$. In Eqs. (V.38) and (V.39) we assume again that the continuum states are energy normalized, $\langle l\,|\,l'\rangle=\delta(l-l')$.

The solutions of the algebraic Eqs. (IV.6) and (IV.7) with (V.38) or (V.39) is straightforward but lengthy and we shall just quote the final results. Most important, we have found that the final vibrational distribution of the products is given by the same form as Eq. (V.37) irrespective of the special form used for the intercontinuum coupling, except that the matrix $\mathbf{F}=\{F(v,k)\}$ is different for each case. This result manifests a special case of the general features of sequential decay involving adjacent coupled continua which will be considered in subsequent work.[20]

For the exponential attenuation, Eq. (V.38), we obtain

$$F(v,k)=\sqrt{\frac{k!}{v!}}\,\frac{Q_v\bar{Q}_k}{Q_N}\,\beta_0^{k-v}\exp\left[-\frac{\phi(k-v)(k+v-1)}{2}\right],\qquad v\le k$$

$$=\sqrt{\frac{v!}{k!}}\,\frac{Q_k\bar{Q}_v}{Q_N}\,(-\beta_0^*)^{v-k}\exp\left[-\frac{\phi(v-k)(v+k-1)}{2}\right],\qquad v\ge k \quad \text{(V.40)}$$

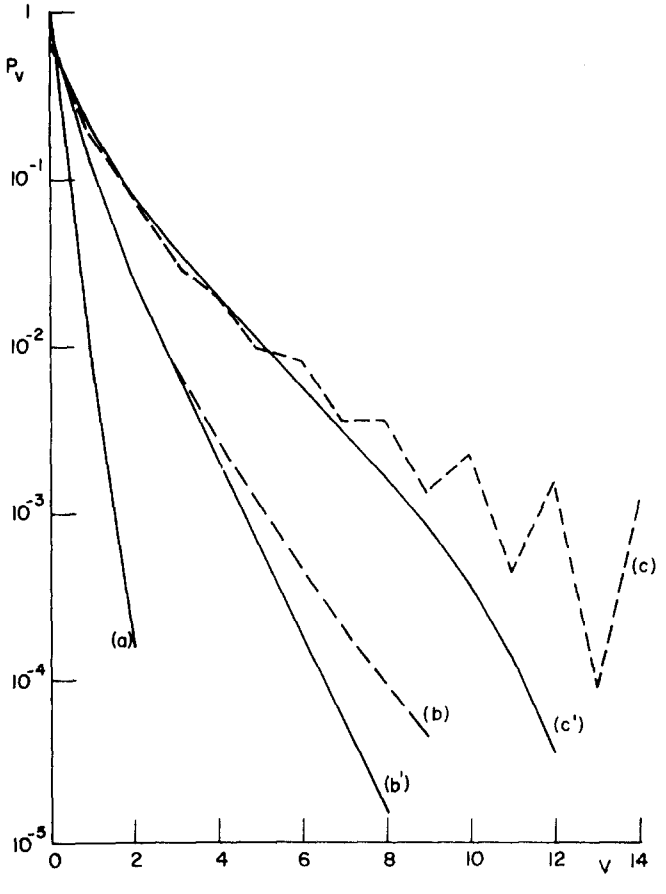

FIG. 13. Effect of the linear attenuation factor q [Eq. (V.39)] on the vibrational distribution for weak coupling. $N=15$. (a) $|\beta|=0.1$ $q=0$, 0.99, (b) $|\beta|=0.5$ $q=0$, (b′) $|\beta|=0.5$ $q=0.99$, (c) $|\beta|=1$ $q=0$, (c′) $|\beta|=1$ $q=0.99$.

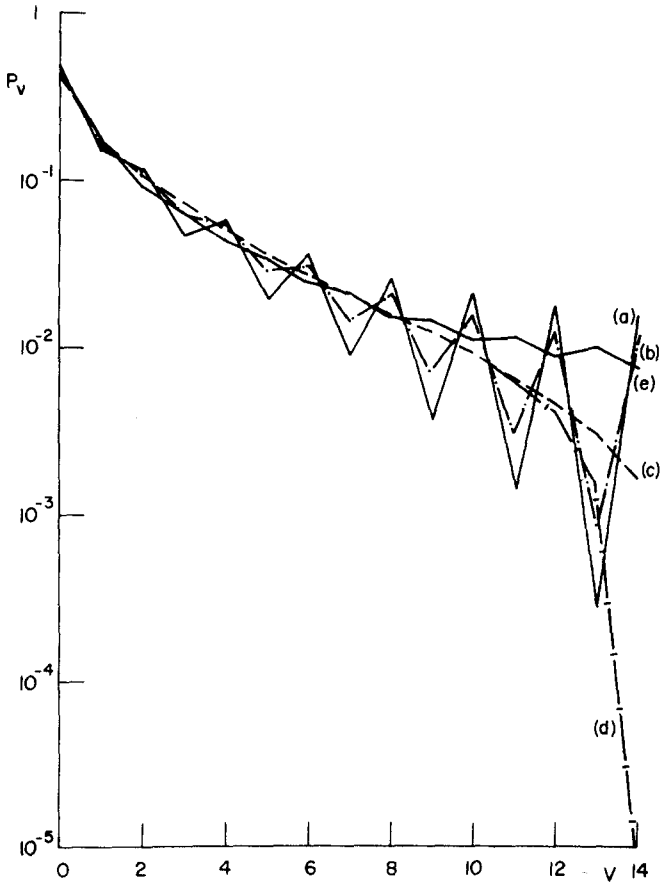

FIG. 14. Effect of the linear attenuation factor q, [Eq. (V.39)] on the vibrational distribution for strong coupling $N=15$. (a) $q=0$, (b) $q=0.5$, (c) $q=0.9$, (d) $q=0.99$, (e) $q=0$ (averaged distribution $\langle P_v\rangle$ for $N=14$ and $N=15$ [Eq. (V.23)].

where $\beta_0=-i\pi\alpha_0\rho_l$ and the polynomials $Q_v,\bar{Q}_v$ are defined in terms of the recurrence relations

$$Q_0=Q_1=1\ ,$$
$$Q_{v+1}=Q_v+|\beta_0|^2 v\exp[-2(v-1)\phi]Q_{v-1}\ ,\quad v\ge 1 \quad \text{(V.41)}$$
$$\bar{Q}_{N-1}=\bar{Q}_{N-2}=1\ ,$$
$$\bar{Q}_{v-1}=\bar{Q}_v+|\beta_0|^2(v+1)\exp(-2v\phi)\bar{Q}_{v+1}(v+1)\ ,\quad v\le N-2\ . \quad \text{(V.42)}$$

For the case of linear attenuation of the coupling, Eq. (V.39), we get

$$F(v,k)=\frac{Q_v\bar{Q}_k}{Q_N}\,\beta_0^{k-v}\prod_{j=v}^{k-1}\left(1-\frac{q}{N-2}j\right)\sqrt{\frac{k!}{v!}}\ ,\qquad v<k$$

$$=\frac{Q_k\bar{Q}_v}{Q_N}\,(-\beta_0^*)^{v-k}\prod_{j=k}^{v-1}\left(1-\frac{q}{N-2}j\right)\sqrt{\frac{v!}{k!}}\ ,\qquad v>k$$

$$=\frac{Q_k\bar{Q}_k}{Q_N}\qquad v=k \quad \text{(V.43)}$$

where $\beta_0=-i\pi\alpha_0\rho_l$, and now the polynomials Q_v and $\bar{Q}_v$ satisfy the following recurrence relations:

$$Q_0 = Q_1 = 1$$

$$Q_{v+1} = Q_v + |\beta_0|^2 v \left[1 - \frac{q}{N-2}(v-1)\right]^2 Q_{v-1}, \quad v \geq 1 \tag{V.44}$$

$$\overline{Q}_{N-1} = \overline{Q}_{N-2} = 1$$

$$\overline{Q}_{v-1} = \overline{Q}_v + |\beta_0|^2 (v+1)\left[1 - \frac{q}{N-2} v\right]^2 \overline{Q}_{v+1}, \quad v \leq N-2 . \tag{V.45}$$

In Figs. 13 and 14 we present the results of numerical calculations for the final vibrational distribution of the products for the linear attenuation model based on Eqs. (IV.6)–(IV.7), and (V.43)–(V.45). The additional parameter which enters into these calculations is the total attenuation factor $\epsilon = 1 - q$. From these results we conclude that:

(a) In the weak coupling limit P_v is not sensitive to the magnitude of the attenuation factor (see Fig. 13).

(b) In the strong coupling limit, reasobable values of $\xi \cong 0.1 - 0.01$ result in damping of the oscillations in P_v. The distribution thus obtained (see Fig. 14) is very similar to that given by the average value $\langle P_v \rangle$ Eq. (V.23). The only difference between the present results and those for $\langle P_v \rangle$ involve "edge effects" for the population of the continua $N-2$ and $N-1$ where P_v drops sharply for small ξ.

(c) The width Γ_g is considerably affected by ξ as is evident from Fig. 15.

This concludes our formal discussion and we now proceed to compare the results of the admittedly approximate theory with the available experimental data.

VI. COMPARISON WITH EXPERIMENTAL RESULTS

We now apply our model to direct photodissociation and predissociation of Cyano triatomic molecules XCN,

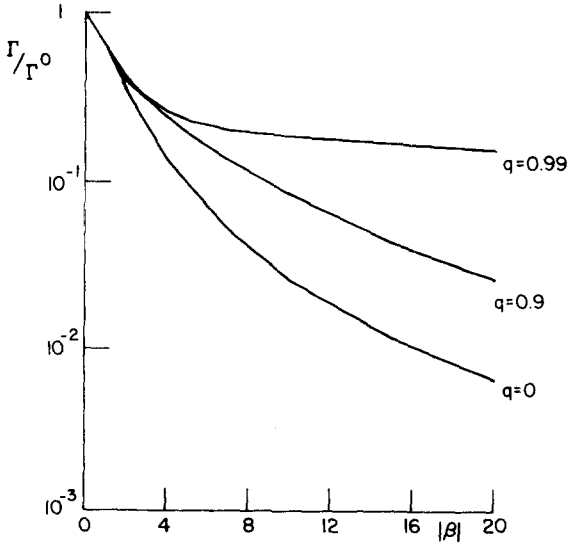

FIG. 15. Effect of the linear attenuation factor [Eq. (V.39)] on the characteristic width. [Eq. (V.16)] $N=8$, $k=0$.

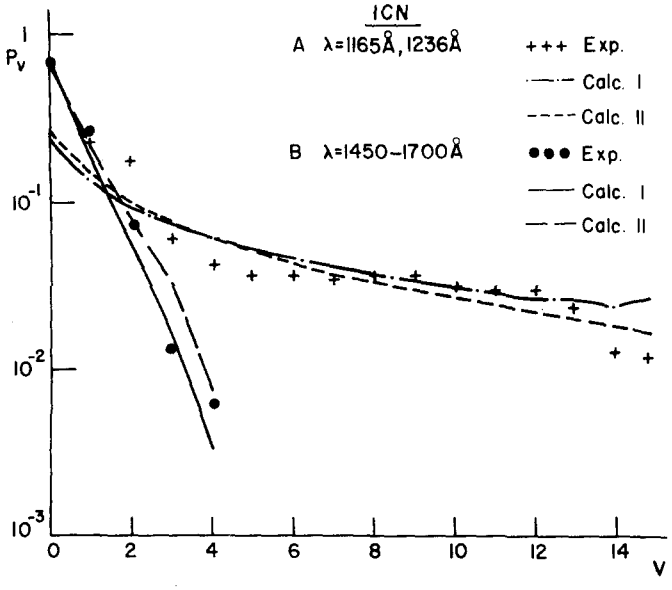

FIG. 16. Comparison of our model with experimental results for ICN.[2]

A.	$N=16$	$\eta=0$	
	Calc I	$\|\beta\|=4$	$q=0.93$
	Calc II	$\|\beta\|=3.5$	$q=0.93$
B.	$N=6$	$\eta=0$	
	Calc I	$\|\beta\|=0.7$	$q=0.9$
	Calc II	$\|\beta\|=0.9$	$q=0.99$

yielding the $B^2\Sigma$ excited state of the CN radical.[2] The compounds studied by Mele and Okake[2] were ICN, BrCN, ClCN, and HCN. Our model is applicable to linear photofragmentation of triatomics and we shall thus consider only the first three molecules. Excitation into the α continuum of these molecules corresponds to direct photodissociation, while excitation at higher energies (below ~1700 Å for ICN, below ~1500 Å for BrCN and below ~1400 Å for ClCN) results in predissociation through Rydberg states.

Utilizing Eqs. (V.27) and (V.37) together with the linear attenuation scheme [Eqs. (V.39), and (V.43)–(V.45)] we notice that four parameters N, η, β, and ξ enter into our theory. The number N of effectively coupled continua was estimated from the excess electronic energy (E_e) above the dissociation threshold (E_t), i.e., $N = (E_e - E_t)/\hbar W_{CN}$, where W_{CN} = is the vibrational frequency of the CN $B^2\Sigma$ radical (see Table I). The parameter η [Eq. (III.20)] determines the vector $\mathbf{V}$ Eq. (V.28), of the Franck–Condon factors. For the case of direct photodissociation η is determined by the configurational change in the internuclear C–N distance between the ground state of XCN and of CN$(B^2\Sigma)$. For predissociation, η is given in terms of the change in the equilibrium distance of XCN in the relevant Rydberg state and of the CN$(B^2\Sigma)$ radical. The available experimental data are summarized in Table I. From these results we conclude that for all cases of interest $\eta = 0.2-1.2$. For $\eta < 0.6$ effective initial coupling occurs practically only to the $v=0$ state and the final vibrational distribution is determined by the intercontinua coupling. For larger η the experimental value was explicitly included.

TABLE I. Energetic and structural data for photofragmentation of XCN compounds.[2,12]

Molecule	Excitation energy $\langle E_e \rangle$ (eV)	Excited state	Nature of photofragmentation	$\langle \Delta E \rangle = \langle E_e \rangle - E_t$ (eV)	N	R_e[a] (Å)	η
ICN	6.7	α	Photodissociation	0.39	2	1.159	0.2
	7.2–8.5	B	Predissociation	1.43	6	1.169	0.4
		C	Predissociation			1.183	0.6
		D	Predissociation				
	8.4, 9.5	G	Predissociation	2.1	9		
		D	Predissociation				
	10, 10.6	High Rydberg states	Predissociation	3.9	16		
BrCN	7.2–8.5	B	Predissociation	0.99	4–5	1.16	0.2
		C	Predissociation			1.185	0.7
		(α)	Photodissociation			1.158	0.15
	8.4, 9.5	B	Predissociation	1.71	7	1.16	0.2
		C	Predissociation			1.185	0.7
		E	Predissociation				
	10, 10.6	High Rydberg states	Predissociation	3.48	14		
ClCN	7.2–8.5	α	Photodissociation	0.99	4–5	1.159	0.2
	8.4, 9.5	B	Predissociation	1.10	5	1.210	1.2
		C	Predissociation			1.213	1.2
	10, 10.6	High Rydberg states	Predissociation	2.88	12		

[a] R_e is the CN equilibrium distance. For photodissociation R_e refers to the ground state of the XCN molecule, for predissociation R_e refers to the predissociating level.

The attenuation parameter was taken in the region $\xi = 0.1 - 0.01$. Except for the final distribution in the $N-1$ and the $N-2$ continua the results are not sensitive to the choice of ξ in the above region. Finally the effective coupling strength β_0 was adjusted to provide best fit to experiment. β_0 corresponds to $\langle 0l \mid v \mid 1l \rangle \rho_l$, i.e., to the product of the coupling between the first pair of continua multiplied by the density of states.

In Figs. 16, 17 and 18 we provide a direct comparison between the theoretical results and the experimental data. Our theoretical scheme faithfully reproduces the experimental behavior of P_v. The general features of these results are: (1) The P_v distribution peaks are at $v = 0$ and (2) the distribution is wider with increasing the photon energy. Feature (1) is consistent with the relatively small value of η which according to the present theory results in initial coupling only to the lowest v values. Feature (2) implies a higher $|\beta|$ value with increasing the excess energy above the dissociation threshold, which is compatible with simple models for intercontinuum coupling.[21] It should be borne in mind that our collinear model is applicable only for photofragmentations of ABC molecules where all electronic states involved have a collinear equilibrium configuration. This is probably the case for the XCN molecules although we cannot ignore the possibility that the electronic state related to the α continuum may be bent.[12] The HCN molecule is linear in its ground state but highly bent in its lowest excited states.[22] In spite of this it is tempting to examine qualitatively this system in the light of the present model hoping that the vibrational distribution is not appreciably affected by the bending. Figure 19 shows the fit of our model to the experimental re-

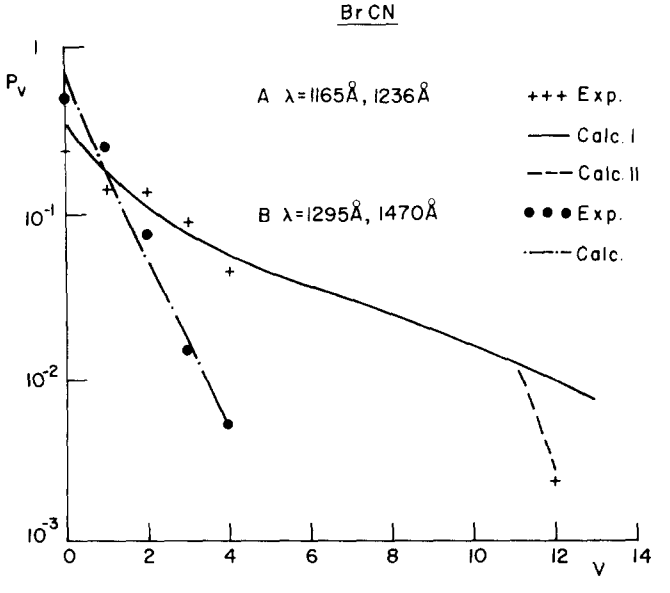

FIG. 17. Comparison of our model with experimental results for BrCN[2]

A. $\eta = 0$

Calc I	$N = 14$	$\lvert\beta\rvert = 2.5$	$q = 0.9$
Calc II	$N = 13$	$\lvert\beta\rvert = 2.5$	$q = 0.95$

B. $N = 7$, $|\beta| = 0.7$ $q = 0.9$ $\eta = 0$.

sults.[2] We expect that for DCN β will be smaller by a factor of 2 as compared to the β value for HCN (since $\beta \sim 1/m$) and so we except the vibrational distribution in the photofragmentation of DCN to be narrower.

Finally, we would like to emphasize that our treatment is applicable only for a collinear photofragmentation process and does not incorporate rotational excitations. The success of our model in accounting for the features of photodissociation of linear triatomics (and also for HCN) may originate from the fact that the statistical approximation for rotation effects[23] may be not too bad for the present case. Thus rotational effects will probably not affect the gross features of the relative vibrational distribution calculated herein. This assumption can be crucially checked by a complete solution of the three dimensional scattering problem with an angular dependent potential.

Summing up this discussion we would like to point out that the results of the present quantum mechanical model for photofragmentation differ from the predictions of the semiclassical "half collision" model.[8] The broad P_v distribution experimentally observed in the photodissociation and predissociation of XCN molecules deviates from a Poisson type or from a quasi-Poissonic distribution,[8] but concurs with the predictions of our model.

APPENDIX A: SOME ALGEBRAIC MANIPULATIONS

We consider the solution of Eqs. (V8)–(V10). Let us try a solution of the form

$$A_v = A_0 \beta^{-v} Q_v / \sqrt{v!}\,, \qquad v \le k \tag{A1a}$$

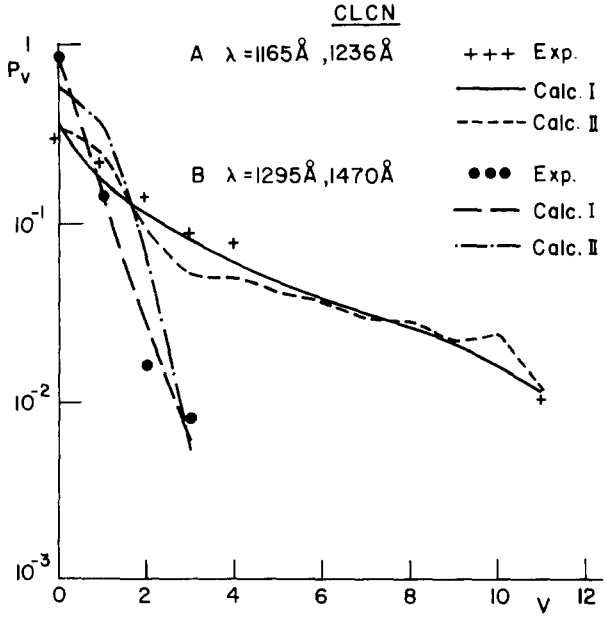

FIG. 18. Comparison of our model with experimental results for ClCN.[2]

A	$N=12$			
	Calc I	$\lvert\beta\rvert=2.5$	$q=0.9$	$\eta=0$
	Calc II	$\lvert\beta\rvert=3$	$q=0.93$	$\eta=1$
B	$N=5$			
	Calc I	$\lvert\beta\rvert=0.5$	$q=0.5$	$\eta=0$
	Calc II	$\lvert\beta\rvert=0.5$	$q=0.97$	$\eta=1$

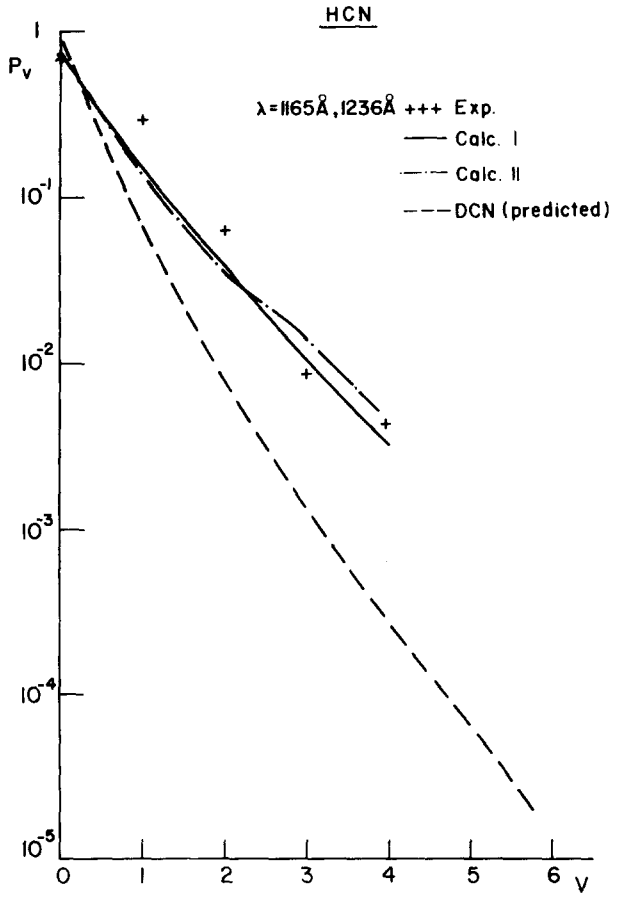

FIG. 19. Comparison of our model with experimental results for HCN.[2]

Calc I	$\lvert\beta\rvert=0.6$	$q=0.9$	$\eta=0$
Calc II	$\lvert\beta\rvert=0.6$	$q=0$	$\eta=0$
DCN	$\lvert\beta\rvert=0.3$	$q=0$	$\eta=0$

$$A_v = \frac{A_{N-1}(-\beta^*)^{v-N+1}\sqrt{v!}}{\sqrt{(N-1)!}}\,\overline{Q}_v\,, \qquad v \ge k \tag{A1b}$$

where $Q_v, \overline{Q}_v$ are some yet unspecified functions of v to be determined by Eqs. (V8)–(V10). Substituting Eqs. (A1) in Eqs. (V8) shows that for $v = 0, 1, \ldots, k-1$ Eqs. (V8) are valid provided that

$$Q_0 = Q_1 = 1 \tag{A2a}$$

and

$$Q_{v+1} = Q_v + \lvert\beta\rvert^2 v Q_{v-1}\,, \qquad v \ge 1 \tag{A2b}$$

in the same way, for $v = N-1, N-2, \ldots, k+1$ the solution (V6) is valid provided that

$$\overline{Q}_{N-1} = \overline{Q}_{N-2} = 1 \tag{A3a}$$

$$\overline{Q}_{v-1} = \overline{Q}_v + \lvert\beta\rvert^2 (v+1)\overline{Q}_{v+1}\,, \qquad v \le N-2\,. \tag{A3b}$$

We have now three different equations regarding A_k:

(1) Using our recursion formula (A2),

$$A_{k-1} = \beta\sqrt{k}\,A_k - \beta^*\sqrt{k-1}\,A_{k-2} \tag{A4}$$

which using (A1) and (A2) gives for A_k:

$$A_k = \frac{A_0 \beta^{-k} Q_k}{\sqrt{k!}}\,. \tag{A4'}$$

(2) Using our recursion formula (A3)

$$A_{k+1} = \beta\sqrt{k+2}\, A_{k+2} - \beta^* \sqrt{k+1}\, A_k \tag{A5}$$

which using Eqs. (A1) and (A3) gives

$$A_k = \frac{A_{N-1}(-\beta^*)^{k-N+1}\sqrt{k!}\ \bar{Q}_k}{\sqrt{(N-1)!}} \ . \tag{A5'}$$

(3) Equation (V9).

In addition we have to satisfy Eq. (V10) which we did not consider yet. We have thus obtained the following four equations for the unknowns $A_0, A_k, A_{N-1}, G^+_{gg}$.

$$A_k = A_0 \beta^{-k} Q_k/\sqrt{k!} \ , \tag{A6}$$

$$A_k = \frac{A_{N-1}(-\beta^*)^{v-N+1}\sqrt{k!}\ \bar{Q}_k}{\sqrt{(N-1)!}} \ , \tag{A7}$$

$$A_k = \frac{-(k+1)|\beta|^2(-\beta^*)^{k-N+1}\sqrt{k!}\ \bar{Q}_{k+1}}{\sqrt{(N-1)!}}\ A_{N-1} \tag{A8}$$

$$- \frac{k|\beta|^2\beta^{-k}Q_{k-1}}{\sqrt{k!}}\ A_0 - \gamma_k \ ,$$

and

$$(E^+ - E_g)\, G^+_{gg} = 1 + V_{g,k} A_k \ . \tag{A9}$$

Solving for A_0 and A_{N-1} we get

$$A_0 = \frac{-\gamma_k\, \bar{Q}_k \beta^k \sqrt{k!}}{Q_{k+1}\bar{Q}_k + (k+1)|\beta|^2 Q_k \bar{Q}_{k+1}}$$

$$\equiv \frac{-\gamma_k \bar{Q}_k \beta^k \sqrt{k!}}{F_N(k)} \tag{A10a}$$

and

$$A_{N-1} = \frac{(-\beta^*)^{N-1}\sqrt{(N-1)!}\ Q_k(-1)^k}{\bar{Q}_k k!\,|\beta|^{2k}}\ A_0 \tag{A10b}$$

it can be easily shown that $F_N(k)$ defined by (A10a) is independent on k. Using Eqs. (A2) and (A3) we have

$$F_N(k) \equiv Q_{k+1}\bar{Q}_k + (k+1)|\beta|^2 Q_k \bar{Q}_{k+1}$$
$$= (Q_k + |\beta|^2 k\, Q_{k-1})\bar{Q}_k + (k+1)|\beta|^2 Q_k \bar{Q}_{k+1}$$
$$= Q_k(\bar{Q}_k + |\beta|^2 (k+1)\bar{Q}_{k+1}) + \bar{Q}_k Q_{k-1}|\beta|^2 k$$
$$= Q_k \bar{Q}_{k-1} + |\beta|^2 k\, Q_{k-1}\bar{Q}_k = F_N(k-1) \ , \tag{A11}$$

and so

$$F_N(k) = F_N(0) = F_N(N-1) = \bar{Q}_{-1} = Q_N \ . \tag{A12}$$

From Eqs. (A10) and (A12) we get for A_0:

$$A_0 = \frac{-\gamma_k \bar{Q}_k \beta^k \sqrt{k!}}{Q_N} \ . \tag{A13}$$

Using (A13) it is straightforward to obtain A_k, A_{N-1}, and G^+_{kk}. Utilization of Eqs. (A6), (A7), and (A9) results in

$$A_k = A_0 \beta^{-k} Q_k/\sqrt{k!} \ , \tag{A14}$$

$$A_{N-1} = \frac{-\gamma_k Q_k \sqrt{(N-1)!}\ (-\beta^*)^{N-k-1}}{Q_N\sqrt{k!}} \ , \tag{A15}$$

$$G^+_{gg}(E) = [E - E_g + i\pi |V_{g,k}|^2 (Q_k \bar{Q}_k/Q_N)\rho_l]^{-1} \ . \tag{A16}$$

Equations (A13)–(A16) were used in Sec. V.

Finally we shall give here the explicit forms of some of the polynomials Q_v and $\bar{Q}_v$:

$$Q_0 = 1 \ ,$$
$$Q_1 = 1 \ ,$$
$$Q_2 = 1 + |\beta|^2 \ ,$$
$$Q_3 = 1 + 3|\beta|^2 \ ,$$
$$Q_4 = 1 + 6|\beta|^2 + 3|\beta|^4 \ ,$$
$$Q_5 = 1 + 10|\beta|^2 + 15|\beta|^4 \ , \tag{A17}$$
$$\bar{Q}_{N-1} = 1 \ ,$$
$$\bar{Q}_{N-2} = 1 \ ,$$
$$\bar{Q}_{N-3} = 1 + (N-1)|\beta|^2 \ ,$$
$$\bar{Q}_{N-4} = 1 + (2N-3)|\beta|^2 \ ,$$
$$\bar{Q}_{N-5} = 1 + 3(N-2)|\beta|^2 + (N-1)(N-3)|\beta|^4 \ ,$$
$$\bar{Q}_{N-6} = 1 + 2(N-4)|\beta|^2 + (2N^2 - 13N + 14)|\beta|^4 \ . \tag{A18}$$

[1] (a) For a detailed list of references concerning photodissociation and predissociation see: G. Herzberg *Molecular Spectra and Molecular Structure, Spectra of Diatomic Molecules* (Van Nostrand, Toronto, 1950); *Electronic Spectra and Electronic Structure of Polyatomic Molecules* (Van Nostrand, Toronto, 1966); (b) N. Basco, J. E. Nicholas, and G. W. Norrish, Proc. R. Soc. A **268**, 291 (1962); **272**, 147 (1963); (c) T. Carrington, J. Chem. Phys. **41**, 2102 (1964); (d) R. W. Diesen, J. C. Wahr, and S. E. Adler, *ibid.* **50**, 3635 (1969); (e) C. Jonah, P. Chandra, and R. Bersohn, *ibid.* **55**, 1903 (1971). (f) G. E. Busch and K. R. Wilson, J. Chem. Phys. **56**, 3626, 3638, 3655 (1972).

[2] A. Mele and H. Okabe, J. Chem. Phys. **51**, 4798 (1969).

[3] (a) R. A. Harris, J. Chem. Phys. **39**, 978 (1963); (b) S. A. Rice, I. Mclaughlin, and J. Jortner, J. Chem. Phys. **49**, 2756 (1968).

[4] B. W. Shore, Rev. Mod. Phys. **39**, 439 (1967).

[5] M. L. Goldberger and R. M. Watson, *Collision Theory* (Wiley, New York, 1969).

[6] (a) U. Fano, Phys. Rev. **124**, 1866 (1961); (b) G. Herzberg, J. Chim. Phys. Special issue "Transitions Non Radiatives dans les Molecules", p. 56 (1970).

[7] G. C. Schatz and A. Kuppermann, J. Chem. Phys. **59**, 964 (1973).

[8] (a) K. E. Holdy L. C. Klotz, and K. R. Wilson, J. Chem. Phys. **52**, 4588 (1970); (b) F. E. Heidrich, K. R. Wilson, and D. Rapp, *ibid.* **54**, 3885 (1971).

[9] M. Shapiro and R. D. Levine, Chem. Phys. Lett. **5**, 499 (1970).

[10] D. Secret and B. R. Johnson, J. Chem. Phys. **45**, 4556 (1966).

[11] J. A. Coxon, D. W. Setser, and W. H. Duewer, J. Chem. Phys. **58**, 2244 (1973).

[12] G. W. King and A. W. Richardson, J. Mol. Spectry. **21**, 339; 353 (1966).

[13] S. Mukamel and J. Jortner, Mol. Phys. (to be published).

[14] (a) G. Karl, P. Kruss, and J. C. Polany, J. Chem. Phys. **46**, 224 (1967); (b) G. Karl, P. Kruus, J. C. Polany, and I. W. M. Smith, *ibid.* **46**, 224 (1967); (c) H. Heydtmann, J. C. Polany, and R. T. Taguchi, Appl. Opt. **10**, 1755 (1971).

[15] (a) J. Comer and F. H. Read, J. Phys. B **4**, 368 (1971); (b) **4**, 1055 (1971).

[16] C. Cohen and Tannoudji, "Theorie des Processus Elementaires d'Interaction entre les Atomes et le Champ Electromagnetique".

[17] J. Jortner and S. Mukamel "Preparation and decay of excited molecular states," *Proceedings of the First International Congress of Quantum Chemistry*, edited by R. Daudel and B. Pullman (to be published).

[18] This propensity rule for the coupling between continua can also be obtained by using the (x, y) coordinate system [Eq. (III. 4)] and expanding $V(x, y)$ to first order in y, which results in $V(x-y) = V(x, 0) + (\partial v/\partial y)_{y=0}\, y$. The formal aspects of the treatment remain invariant, only the interpretation of

β has now to be modified. Such an approach may be useful for the study of photodissociation of polyatomics.

[19](a) A. Nitzan, J. Jortner, and B. Berne, Mol. Phys. **26**, 201 (1973); (b) R. Lefevre and J. A. Beswich, *ibid.* 23, 1223 (1973).

[20]S. Mukamel and J. Jortner (to be published).

[21]To demonstrate this point let us consider a simple model system. For a particle in a box we have

$$\langle l \left| \frac{\partial}{\partial z} \right| l' \rangle \sim \begin{cases} \frac{ll'}{l^2 - l'^2} & l + l' = 2n + 1 \\ 0, & l + l' = 2n \end{cases}$$

where n is an integer. The density of states is $\rho_l \sim 1/l$; $\rho_{l'} \sim 1/l'$ and so $|\beta|^2 \alpha |V_{ll'}|^2 \rho_l \rho_{l'} \alpha ll'/(l^2 - l'^2)^2$. Since we consider resonance coupling, $l^2 - l'^2$ is proportional to the energy difference between the threshold of adjacent continua (which is $\hbar\omega$ irrespective of l and l') and thus $|\beta|^2 \alpha ll'$ which is an increasing function of l and l', and consequently a decreasing function of v and v').

[22]G. Herzberg and K. K. Innes, Can. J. Phys. 35, 842 (1957).

[23]R. D. Levine, *Quantum Mechanics of Molecular Rate Processes* (Oxford U. P., London, 1969).